AD-A151 849 SPECTROSCOPIC STUDIES OF LEAD OXIDE IN A FLOW TUBE(U) 1/1
AIR FORCE INST OF TECH WRIGHT-PATTERSON AFB OH SCHOOL
OF ENGINEERING J P DURAY 03 DEC 84 AFIT/GEP/PH/84D-2
UNCLASSIFIED F/G 7/4 NL

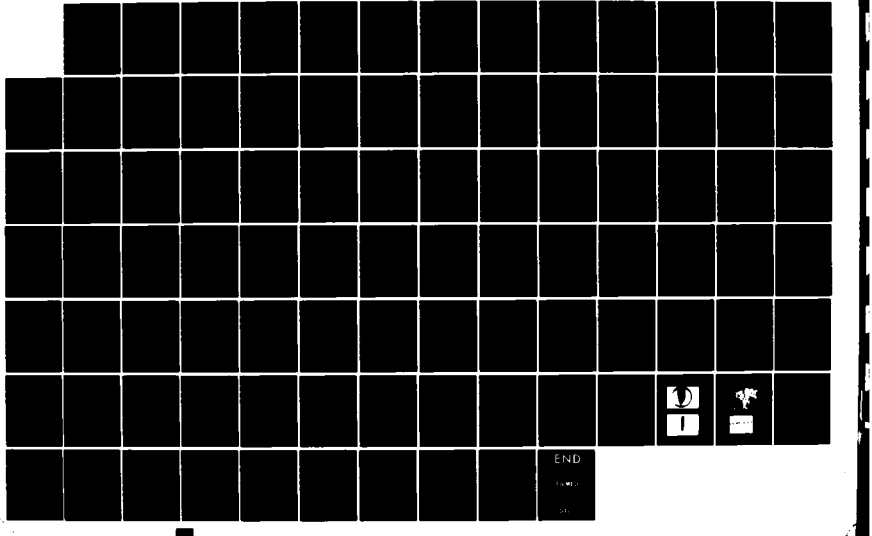

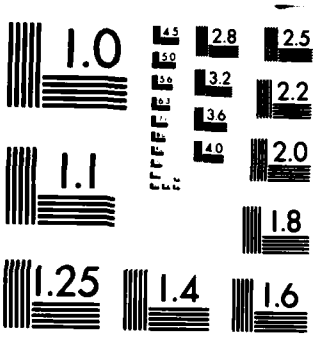

MICROCOPY RESOLUTION TEST CHART
NATIONAL BUREAU OF STANDARDS-1963-A

SPECTROSCOPIC STUDIES OF LEAD OXIDE IN A FLOW TUBE

THESIS

Jeffery P. Duray
Captain, USAF

AFIT/GEP/PH/84D-2

DEPARTMENT OF THE AIR FORCE
AIR UNIVERSITY
AIR FORCE INSTITUTE OF TECHNOLOGY

Wright-Patterson Air Force Base, Ohio

AFIT/GEP/PH/84D-2

SPECTROSCOPIC STUDIES

OF LEAD OXIDE IN A FLOW TUBE

THESIS

Jeffery P. Duray
Captain, USAF

AFIT/GEP/PH/84D-2

AFIT/GEP/PH/84D-2

SPECTROSCOPIC STUDIES OF LEAD OXIDE IN A FLOW TUBE

THESIS

Presented to the Faculty of the School of Engineering

of the Air Force Institute of Technology

Air University

in Partial Fulfillment of the

Requirements for the Degree of

Master of Science

Jeffery P. Duray, B. S.

Captain, USAF

December 1984

Approved for public release; distribution unlimited

Preface

This research is part of an on-going project at AFIT to characterize the chemiluminescence of lead oxide.

I found this project both fun and painful. I have learned much about how to preform spectroscopy and research. I wish I had more time to continue this work since it seems I just got everything going and I had to stop.

Many people have helped me in this project and I would like to thank them. A big thanks goes to my thesis advisor, Dr. Ernest Dorko, for his help and words of encouragement during this project. I would like to thank Carl Shortt and the personnel of the AFIT Fabrication Shop for their excellent work in making parts for the flow-tube system. A thanks goes to Bob Wade for his excellent work on the Pyrex oxidizer head. This project may not have happened without his help. Also, a thanks goes to the guys of the Physics Laboratory; Curt Atnipp, George Gergal ,and Don Elworth for their assistance and advice. Finally, I would like to thank my family and friends for their understanding and support throughout this project.

Jeffery P. Duray

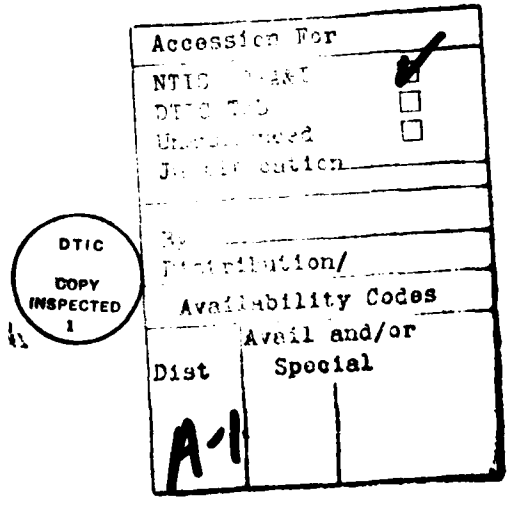

Table of Contents

Table of Contents (continued)

List of Figures

List of Tables

Abstract

Chemiluminescent flame from lead oxide has been observed in a flow-tube reactor. The chemiluminescence was produced by the reaction of lead vapor with singlet delta oxygen, $O_2(^1\Delta)$ first electronically excited state of oxygen. Spectra was recorded using a monochromator and a photo-multiplier tube (PMT). The spectra was recorded from the PMT in the photon counting mode on a Signal Averager (Model 4203 EG&G PAR). The Signal Averager was operated in the multichannel scaling mode which records data in a histogram format.

Analysis of the spectra led to assignments of electronic transitions from a, b, A, C', D, E to the ground state of PbO. Molecular constants were calculated from the combination of this data and previous data taken at the Air Force Institute of Technology. The constants were compared to those of other researchers. The table below lists the molecular constants.

The relative concentrations of excited Pb in the lead vapor were measured by using absorption spectroscopy techniques. The results were inconclusive because of light souce stability problems.

Table of Molecular Constants for PbO

ELECTRONIC STATE	T_e	ω_e	$\omega_e X_e$
X	0	722.69(0.48)	3.613(0.030)
a	16031.1(4.0)	483.4(1.5)	2.71(0.12)
b	16335.4(6.4)	433.5(5.3)	-0.36(0.90)
A	19876.2(3.3)	445.2(1.5)	0.78(0.15)
B	22303.6(4.0)	491.7(2.0)	0.98(0.21)
C	23794.6(5.6)	550.6(2.3)	5.46(0.19)
C'	24941.9(5.9)	500.1(2.1)	3.40(0.15)
D	30059.3(6.9)	617.7(5.0)	9.56(0.80)
E	34443.0(11.2)	477.4(12.8)	13.0(2.6)

All numbers are in cm^{-1}

NOTE: Number in parentheses is one standard deviation

SPECTROSCOPIC STUDIES OF LEAD OXIDE IN A FLOW TUBE

I. Introduction

Background

The Air Force is currently looking for lasers that operate in the ultra-violet part of the electromagnetic spectrum. These shorter wavelength lasers propagate through the atmosphere with less loss than their counterparts in the infrared. Also chemical lasers are being studied for use in high energy applications. Before a high power laser is built, a low power version is developed and tested. Chemical lasers are excellent candidates for high energy applications since at least in principle, a small low power version can easily be tested which then can be scaled up into a high power version by adding more chemical reactants. Other lasers may require large electrical power supplies which are undesirable for military operations.

Lead oxide (PbO) is a possible candidate for a chemical laser because of its chemiluminescence. Previous work at the Air Force Institute of Technology (AFIT) has partially characterized the emission spectrum of PbO. Additional work is required to complete this characterization before the total lasing potential of PbO can be developed. This thesis is to continue the research of the emission spectrum of PbO.

Problem

The objective of this thesis was to study the chemiluminescence of lead vapor combined with singlet delta oxygen, $O_2(^1\Delta)$ (first electronically excited state of oxygen), which forms PbO. Also, the concentrations of Pb in its various excited states were to be determined by

absorption spectroscopy. This experimental data was combined with previous data to upgrade the molecular constants that describe the chemical reaction.

Approach

This was an experimental thesis which used equipment and facilities at AFIT. A previously developed theory was used to analyze the data.

Lead vapor and $O_2(^1\Delta)$ was combined in a flow tube reactor, and the chemiluminescence produced was analyzed using a monochromator and photomultiplier tube (PMT). The flow tube system was the same set-up as used by Ritchey (21). Lead vapor was produced in an electrically heated furnace and brought into the flow tube by an inert gas (argon). $O_2(^1\Delta)$ was produced in a microwave generator and brought to the flow tube under its own pressure.

The absorption spectroscopy techniques were used to try to determine the relative concentrations of lead in the vapor stream. An electrodeless lead lamp was used as the light source.

II. Theory

Introduction

This section discusses the theory of molecular spectroscopy and the application to lead oxide. A brief overview of molecular spectroscopy is presented, followed by the spectroscopy of lead oxide chemiluminescence. Then, the theory of absorption spectroscopy as it relates to the description of concentrations of lead in the chemical reaction is given. Finally, a brief review of recent literature on the spectroscopy of lead oxide is presented.

Molecular Spectroscopy

Molecular spectroscopy is the study of absorption and emission of electromagnetic radiation by molecules. This study involves the experimental measurement of two things, the wavelength of the transition and the relative intensity of the absorption or emission. The information contained in the spectrum is unique for every molecule and can be used to identify the molecule. The experimental data can be used to aid in the understanding of the physics of a molecule.

In this thesis, a diatomic molecule, lead oxide, is investigated. Therefore, the discussions are limited to the case of diatomic molecules. Molecules can be modeled as vibrating and rotating systems. A diatomic molecule can be pictured as an anharmonic oscillator consisting of two masses that represent the elements which are connected by nuclear forces.

The energy of each energy state of a diatomic molecule can be separated by the use of the Born-Oppenheimer approximation into electronic, vibrational and, rotational contributions (6:V1).

$$E_{total} = E_{electronic} + E_{vibration} + E_{rotation} \qquad (1)$$

E = energy

E_{total} = the energy of each energy state

What is measured spectroscopically are the transitions between these possible energy states.

The spectroscopic transitions and the two energy states of energy E_2 and E_1 are related by the Bohr-Einstein law, equation 2 (see Fig 1).

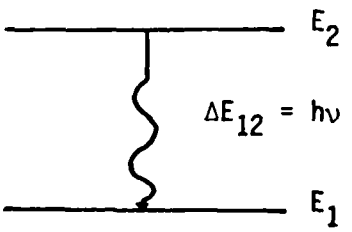

Figure 1. Bohr-Einstein Law

$$\Delta E = h\nu = hc/\lambda = hc\bar{\upsilon} \qquad (2)$$

E = the energy difference between energy states of energy E_2 and E_1

h = Planck's constant

ν = frequency (Hz) of the electromagnetic radiation absorbed of emitted by the molecule

c = speed of light

λ = wavelength (cm)

$\bar{\upsilon}$ = wave number (cm^{-1})

Based on the Born-Oppenheimer approximation a transition can be represented as follows:

$$\Delta E_{total} = \Delta E_{electronic} + \Delta E_{vibration} + \Delta E_{rotation} \qquad (3)$$

Electronic changes can be observed for all diatomic molecules. Inclusion of vibrational changes produces the coarse spectrum for an electronic transition (i.e. the vibronic spectrum) and rotational changes produce the fine spectrum (i.e. the ro-vibronic spectrum). Rotational changes are only observed in high resolution spectroscopy. This thesis reports observations of the vibronic or coarse spectrum of lead oxide. The observed spectral lines are due to transitions from the vibrational energy levels of excited states to the vibrational levels of lower energy states. The transitions are called bands and the band spectrum that vibrational changes produce can be described mathematically as

$$\bar{\upsilon}(v',v'') = Te' + [(v' + 1/2)\,\omega e' - Xe'(v' + 1/2)^2 \omega e'] \quad (4)$$
$$-[(v'' + 1/2)\,\omega e'' - Xe''(v'' + 1/2)^2 \omega e'']$$

$\bar{\upsilon}$ = frequency of the transition (cm^{-1})

Te' = electronic energy separation between ground and excited states

Xe = anharmonicity vibrational constant

ωe = $\omega / 2\pi c$, ω = angular velocity

v = vibrational quantum number

' represents an upper electronic state

'' represents a lower electronic state

There is *no selection rule governing the* vibrational transitions. Therefore, virtually every transition has some probability of occuring if the electronic transition is allowed. Not all transitions are observed or have equal intensity. This can be explained by the Franck-Condon principle and the potential energy curves of two electronic states.

The Franck-Condon principle states that an electronic transition takes place so rapidly that a vibrating molecule does not change its inter-nuclear distance or its momemtum during the transition (6:V11-4). This is shown on the potential energy curve, figure 2, by a "vertical" transition to the lower state. When this happens, the molecule maintains a constant inter-nuclear spacing (r). In figure 2, the v' = 0 to v'' = 2 set of transitions has a high probability of occuring due to the matching of the two curves.

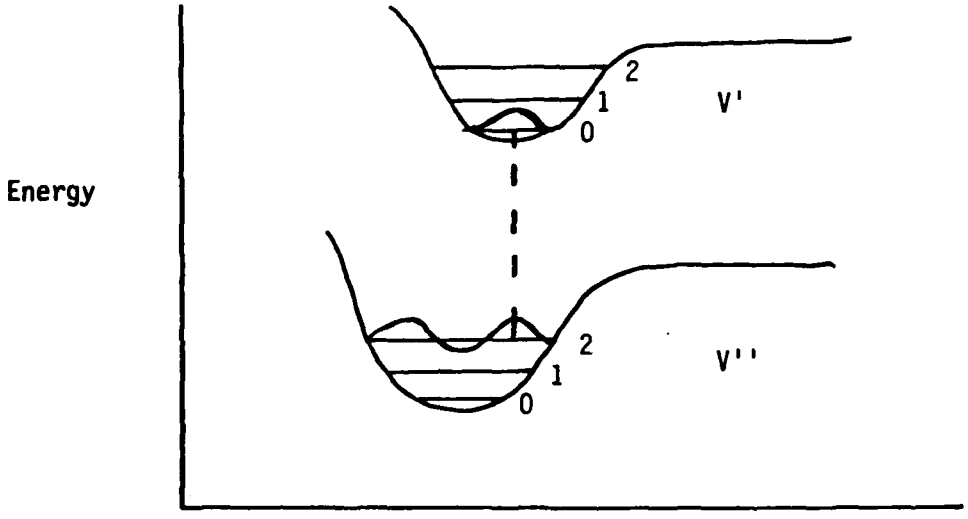

Figure 2. Potential energy curves

The Franck-Condon principle will provide the relative probability of a transition (Franck-Condon factor). Another way to look at this is the wave-mechanical treatment of the Franck-Condon principle. The largest Franck-Condon factor happens when the maxima and mimina in the vibrational eigenfunctions for the two states of interest occur at the same internuclear distance (12:199).

Electronic transitions can be grouped into families called progressions and series. Progressions are transitions from the same upper state to different lower states - called a v'' progression. Simmilarly, v' progressions represent transitions from different higher to the same lower energy state. Series are transitions between upper and lower states that have the same vibrational quantum number.

All the possible vibrational transitions between two electronic levels can be arranged in a Deslandres table (see Figures 14-15). The table is arranged such that v'' progressions form columns, v' progressions form rows, and series form diagonals. With the proper (v',v'') transition

assignments in a Deslandres table, the energy differences between successive pairs in a row will be approximately equal. Similarly, the differences between successive pairs in a column will be approximately equal. This method provides a good way of checking the validity of the assignments of the transitions. Also a comparison of calculated Franck-Condon factors and observed relative intensities is an additional check on the validity of the assignments.

Low resolution spectroscopy will give a vibrational spectrum consisting of a series of broad bands. These bands are due to the unresolved rotational transitions within the vibrational transitions. The bands have a sharply defined edge called a band head where the intensity of the band drops rapidly. On the long wavelength side of the band, the intensity drops slowly and this is called shading. The band head is usually close to the band origin which represents a transition between two rotationless states (12:112).

Spectroscopy of Lead Oxide

Electronically excited lead oxide (PbO^*) can be formed by the reaction of lead vapor, Pb(g), and singlet delta oxygen $O_2(^1\Delta)$ (first excited state of oxygen). Singlet delta oxygen produces a more intense chemiluminescence than ground state oxygen.

TABLE I. Electronic State Energies

STATE	ENERGY (cm^{-1})	REFERENCE
X	0	
a	16030.9	9
b	16340.8	9
A	19873.7	9
B	22298.6	9
C	23793.6	9
C'	24938.9	9
D	30083.0	9
E	34455.0	25

Researchers have observed emissions from eight different electronic states of PbO^* to the ground state (9; 21; 25). These states and their respective energies are shown in Table I. Figure 3 shows the potential energy curves of the different states.

A theoretical picture of lead oxide can be developed by working with the valence electronic configuration of the diatomic molecule. Lead has a $(6s)^2$ $(6p)^2$ valence electronic configuration and oxygen a $(2s)^2$ $(2p)^4$ configuration. The complete ground electronic configuration of lead oxide can be represented using Mulliken's convention as (12):

$$(KKLMNO)\ (Z\sigma)^2\ (Y\sigma)^2\ (\omega\sigma)^4\ (X\sigma)^2$$

or simply as $(\sigma)^2 (\pi)^4$, which indicates a closed valence shell for PbO. The electronic energy states of a molecule can be predicted starting with the electronic configuration from the angular momentum coupling schemes of Hund (12:219-226). There are a number of selection rules between these electronic states that apply to particular cases which are based on the atomic weight and on the symmetry of the molecule. Lead oxide is a heavy molecule and the rules that are applicable are based on Hund's case c coupling (17:396).

These selection rules for case c coupling are:

$$\Delta\Omega = 0, \pm 1; \quad 0^+ \not\leftrightarrow 0^-$$

Ω is the total electronic angular momentum quantum number

Figure 4 shows the electronic configurations correlated with the electronic energy states. The ground state electronic configuration is $\sigma^2 \pi^4$ and the first two excited states are $\pi^3\pi$ and $\sigma\pi$. Transitions are allowed between the excited states and the ground state for all of the observed spectral lines except for the $b0^-$ - $X0^+$ transition which is not allowed in case c coupling since the reflection symmetry rule is violated.

Chemiluminescence

Emission spectra can be observed in many different experimental arrangements. Current interest is in the characterization of spectra observed in chemiluminescence. Chemiluminescence is defined as the emission during the course of a chemical reaction.

Chemiluminescence has been observed during the reaction between Pb and $O_2(^1\Delta)$. The mechanism of this reaction which leads to chemiluminescence has been suggested by Bachar and Rosenwaks on the following sequence of steps (2:530-531):

$$Pb(^3P_1) + O_2(^1\Delta) \rightarrow Pb(^3P_2) + O_2(^3\Sigma) \quad (5)$$

$$Pb(^3P_2) + O_2(^1\Delta) \rightarrow PbO(X,v) + O(^3P) \quad (6)$$

$$PbO(X,v) + O_2(^1\Delta) \rightarrow PbO(a,b) + O_3(^3\Sigma) \quad (7)$$

$$PbO(a,b) + O_2(^1\Delta) \rightarrow PbO(A,B,...) + O_3(^3\Sigma) \quad (8)$$

where PbO(X,v) indicates PbO in vibrationally excited levels of the ground state and PbO(a,b,A,...) represents electronically excited states of PbO. Work done by Ritchey tends to support this mechanism but it is still not fully understood (2; 8; 17, 21). Figure 5 shows the relative positions of the ground and excited energy levels of Pb, O_2, and PbO.

The elements used for the PbO chemilumescence are easily produced. The lead vapor is produced by resistive heating. The excited oxygen is produced in a microwave discharge cavity operating at 2450 MHz. The lead vapor is transported to the reaction area by a flow of Argon gas. The oxygen is delivered to the reaction area under its own pressure. The microwave discharge produces both $O_2(^1\Delta)$ and $O_2(^1\Sigma)$. The lifetime and concentration of $O_2(^1\Delta)$ are at least 10^3 times greater than that for $O_2(^1\Sigma)$ so $O_2(^1\Sigma)$ is not considered to contribute significantly to the reaction mechanism (26:24). Some oxygen atoms are still present after going through the microwave discharge and these atoms are eliminated by passing the gas stream over an HgO coated surface (2:527; 1:2053). $O_2(^1\Delta)$ is quenched rapidly upon contact with metal so Pyrex with a low quenching efficiency is used to carry the gas to the reaction area.

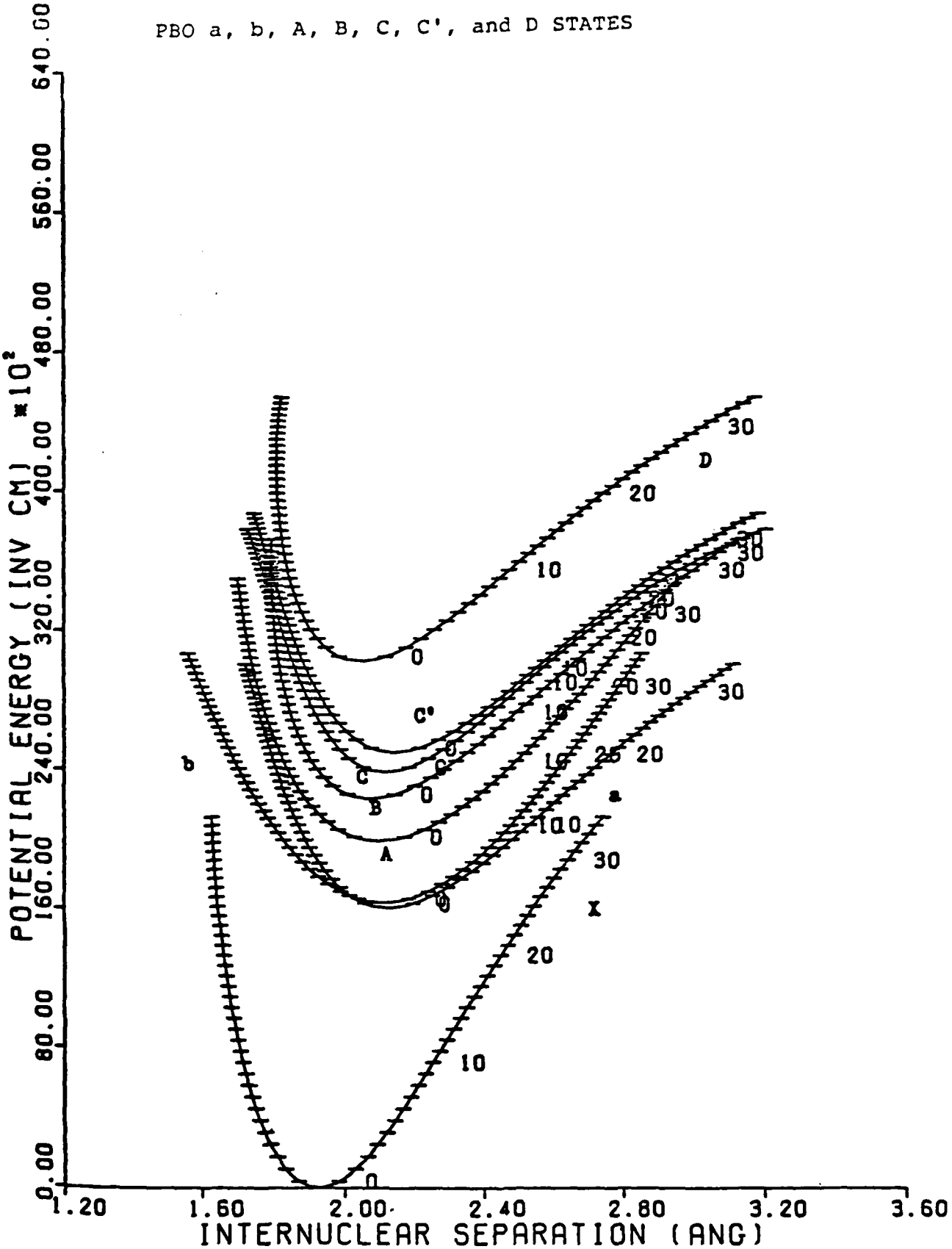

Figure 3. Potential Energy Curves for Different Electronic States of PbO (19)

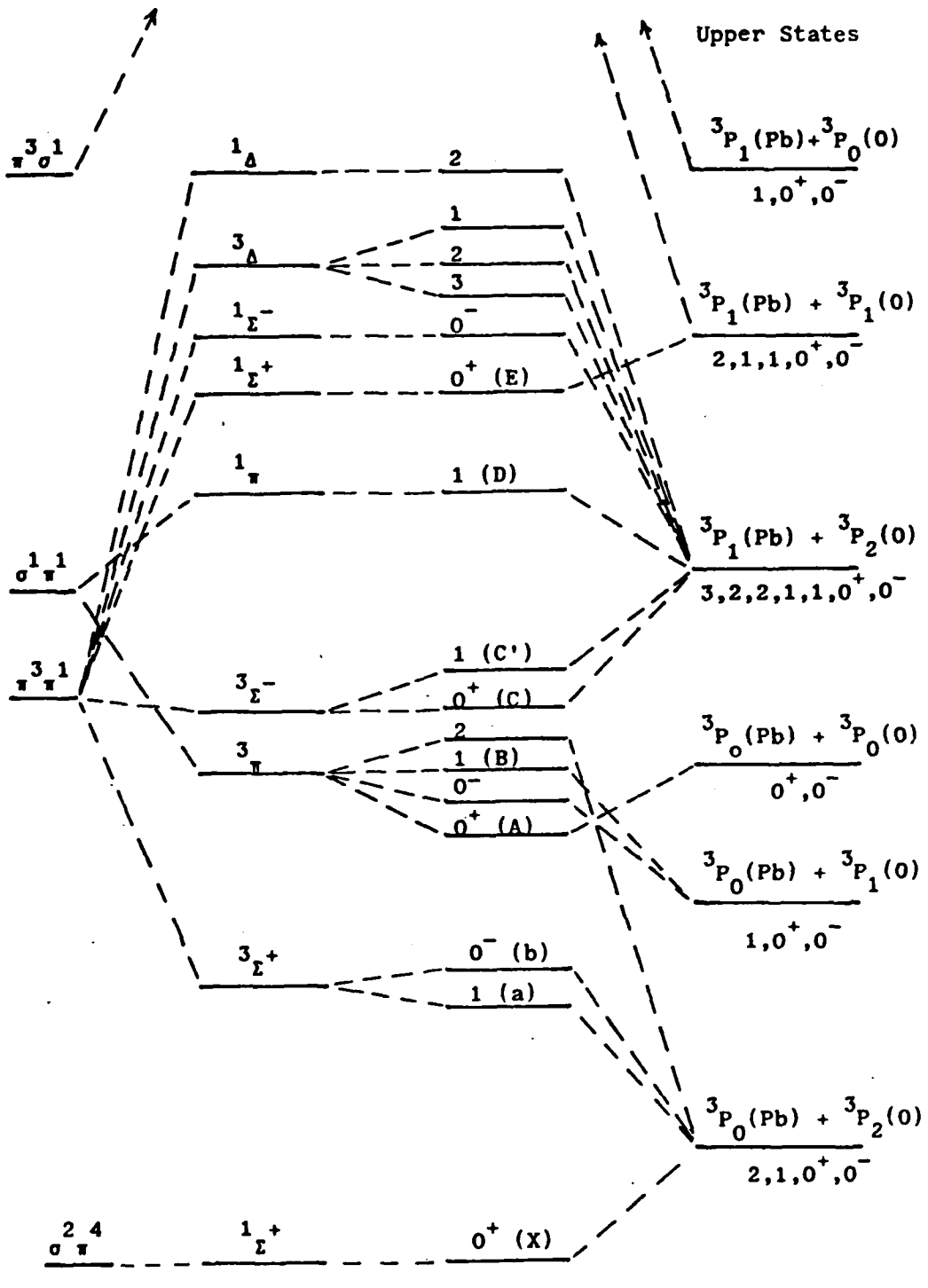

Figure 4. Electronic Configurations Correlated with the Electronic Energy States

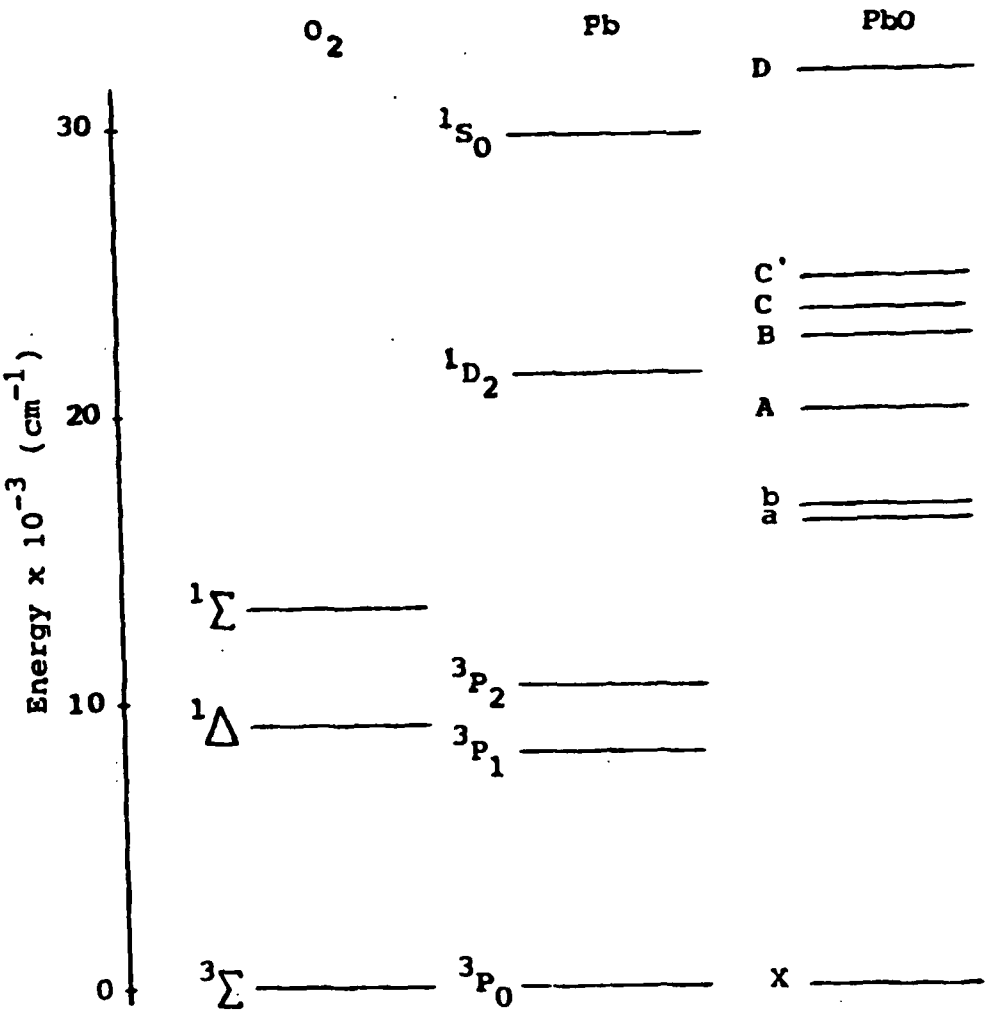

Figure 5. Relative Positions of Excited States of Pb, O_2, and PbO

Absorption Spectroscopy

Absorption spectroscopy can be used to determine the absorption coefficient of a material or the concentrations of a particular substance. Different wavelengths of spectral lines may be absorbed or emitted from a substance. This depends on the chemical make-up of the substance.

The irradiance absorbed in an absorbing region for a spectral line is given by (12:20)

$$E_{abs}^{nm} = E_o^{nm} N_m B_{mn} h \bar{\upsilon}_{nm} \Delta x \qquad (9)$$

E_{abs} = irradiance of absorbed radiation, erg/(s cm^2)

E_o^{nm} = irradiance of incident radiation, erg/(s cm^2)

N_m = number of atoms / cm^3

B_{mn} = Einstein transition probability of absorption (cm^3/erg s)

$\bar{\upsilon}_{mn}$ = wave number of transition (cm^{-1})

Δx = thickness of absorption layer (cm)

m = lower state

n = higher state

B_{mn} is related to the Einstein transition probability of spontaneous emission (A_{mn}) by

$$B_{mn} = A_{nm} / (8 \pi h \bar{\upsilon}_{mn}^3) \qquad (10)$$

Table II Energy Levels of Pb(I) (10:66)

Level	Observed energy (cm^{-1})	Wavelength (Å)
^3P_o	0	--
$^3P_1$	7819	12789
$^3P_2$	10650	9390
$^1D_2$	21458	4660
^1S_o	29467	3394

One assumption is made in the above equations that the wave number interval around $\bar{\upsilon}_{mn}$ is sufficient to cover the whole line width. The natural line width can also affect these equations. This can be neglected when considering a thin absorbing layer (12:19-20) which is done in this thesis since a thin layer of low pressure vapor (1.5 cm, 2 Torr) is used. The irradiance transmitted through an absorbing region can be given by

$$E_t^{nm} = E_o^{nm} \exp(- N_m B_{mn} h \bar{\upsilon}_{nm} \Delta x) \qquad (11)$$

E_t^{nm} = irradiance of transmitted radiation, erg/(s cm^2)

Garstang lists the energy levels and transition probabilities of Pb (10). Tables II and III tabulates these values. A_m is the magnetic dipole transition probability and A_q is the electric quadruple transition probability. The Einstein probability A_{mn} is the sum of the probabilities given for a particular state.

Table III Transition Probabilities for Pb(I) (10:67)

Transition	Type	Probabilities (sec^{-1})
$^1S_o - {}^3P_o$	A_m	80(e)
$^1D_2 - {}^3P_o$	A_q	0.0017
$^3P_2 - {}^3P_o$	A_q	0.21
$^3P_1 - {}^3P_o$	A_m	7.3

(e) estimate

Literature Search

The most recent published work is by Dorko and others (8). They report the chemiluminescence observed during the reaction between Pb and O_2 ($^3\Sigma$). Transitions from the a, A, B, C electronic states to the ground state were observed. A two step mechanism for the reaction is proposed:

$$Pb + O_2 (^3\Sigma) \rightarrow PbO(X) + O(^3P_2) \qquad (12)$$

$$Pb + O(^3P_2) \rightarrow PbO^* \qquad (13)$$

The most recent work done on PbO with the use of O_2 ($^1\Delta$) is reported by Ritchey (21). Ritchey compared the chemiluminescence during the reaction of Pb and O_2 ($^3\Sigma$) to the reaction of Pb and O_2 ($^1\Delta$). He noticed a significant enhancement of the A and B states over the a-state with the use of O_2 ($^1\Delta$). Activation energies for the reaction of Pb + O_2 ($^1\Delta$) were found which experimentally verifies the mechanism proposed by Bachar and Rosenwaks (2).

Extensive literature searches have been performed by Glessner and Ritchey (11; 21). The reader is directed to these searches for additional information. One source not reported in the searches is work done by Johnson. Johnson (14) did spectroscopic studies of a number of metal-oxide molecules using laser excited fluorescence. PbO was looked at in chemiluminescence and fluorescence. Johnson saw transitions for the A, B, and, C states. Lifetime measurements were made on the B states. The set-up he used to produced lead vapor and excited oxygen are similar to the set-up used in the work reported in this thesis. He used a flow-tube system along with a resistively heated furnace for the Pb and a microwave discharge for the production of excited oxygen.

III. Experimental Set-Up

Introduction

The equipment and set-up for the experiments are discussed in this section. Two experiments are described; lead oxide flow-tube chemiluminescence and lead absorption spectroscopy. A complete listing of equipment and materials is given in Appendix A.

Lead Oxide Flow-Tube Chemilumescence

The flow-tube system is basically the same as that used by Ritchey (21). Figure 6 shows the set-up. The system is made up of five components:

1; VACUUM SYSTEM

2; FLOW-TUBE SYSTEM

3; OPTICAL TRAIN

4; DETECTION SYSTEM

5; RECORDING SYSTEM

1; Vacumm System. The vacuum system is made up of two vacuum pumps, 1 1/2 in. inside diameter (ID) steel pipe, 1 1/5 in. ball valve, and 2 7/8 in. ID stainless steel pipe, see figure 7. The pumps are connected together with the 1 1/2 in. pipe and a "Y" connector. The valve is connected to the "Y" by a 1 1/2 in. pipe. Another section of 1 1/2 in. pipe connects the valve to a coupler 1 1/2 in. to 2 7/8 in. The coupler contains 2 outlets for monitoring the pressure. This system was designed by Koym (16). A new vacuum system was designed with the major parts having a diameter of 4 in. , see figure 8.

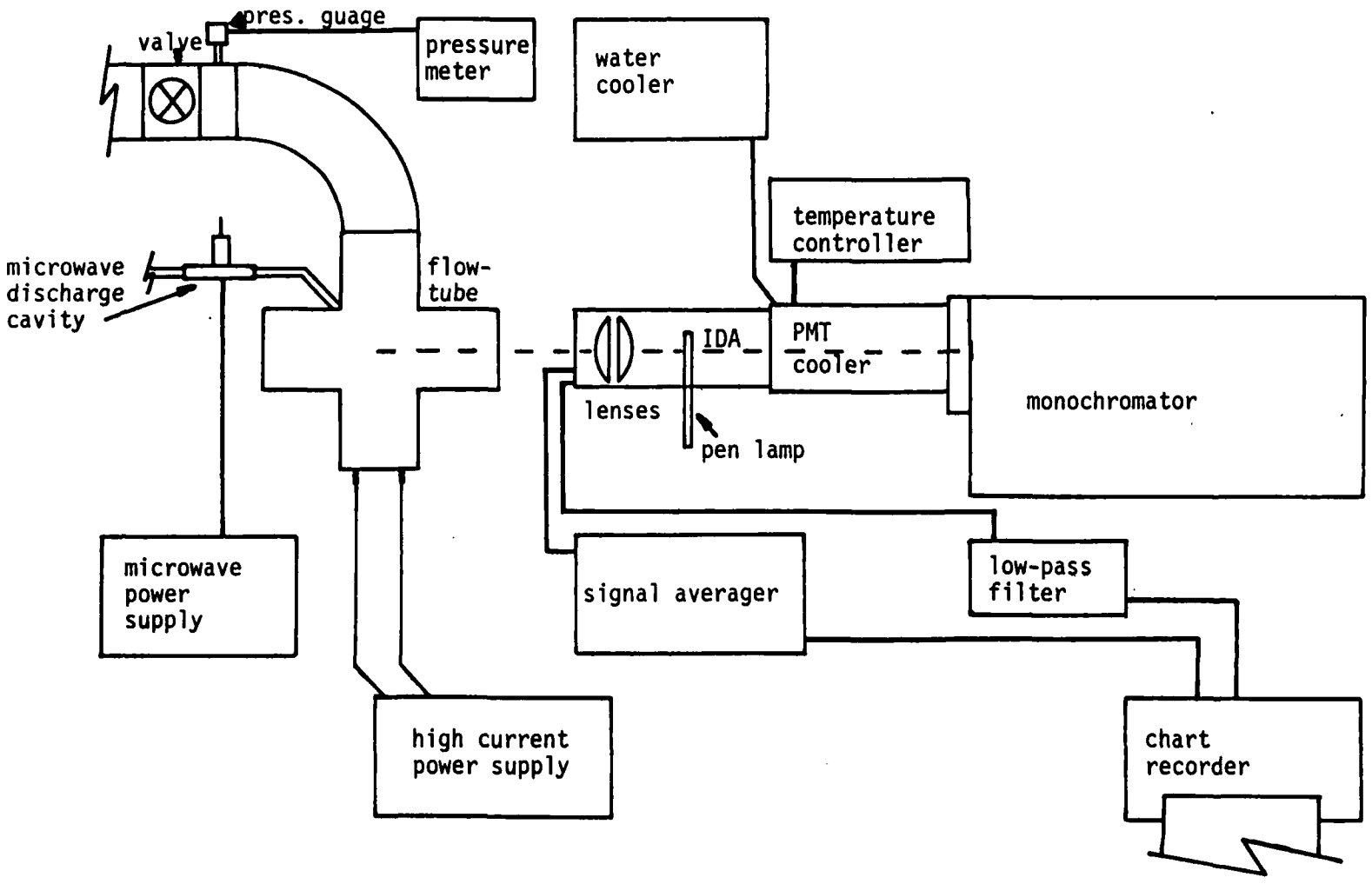

Figure 6. Complete Flow-Tube System

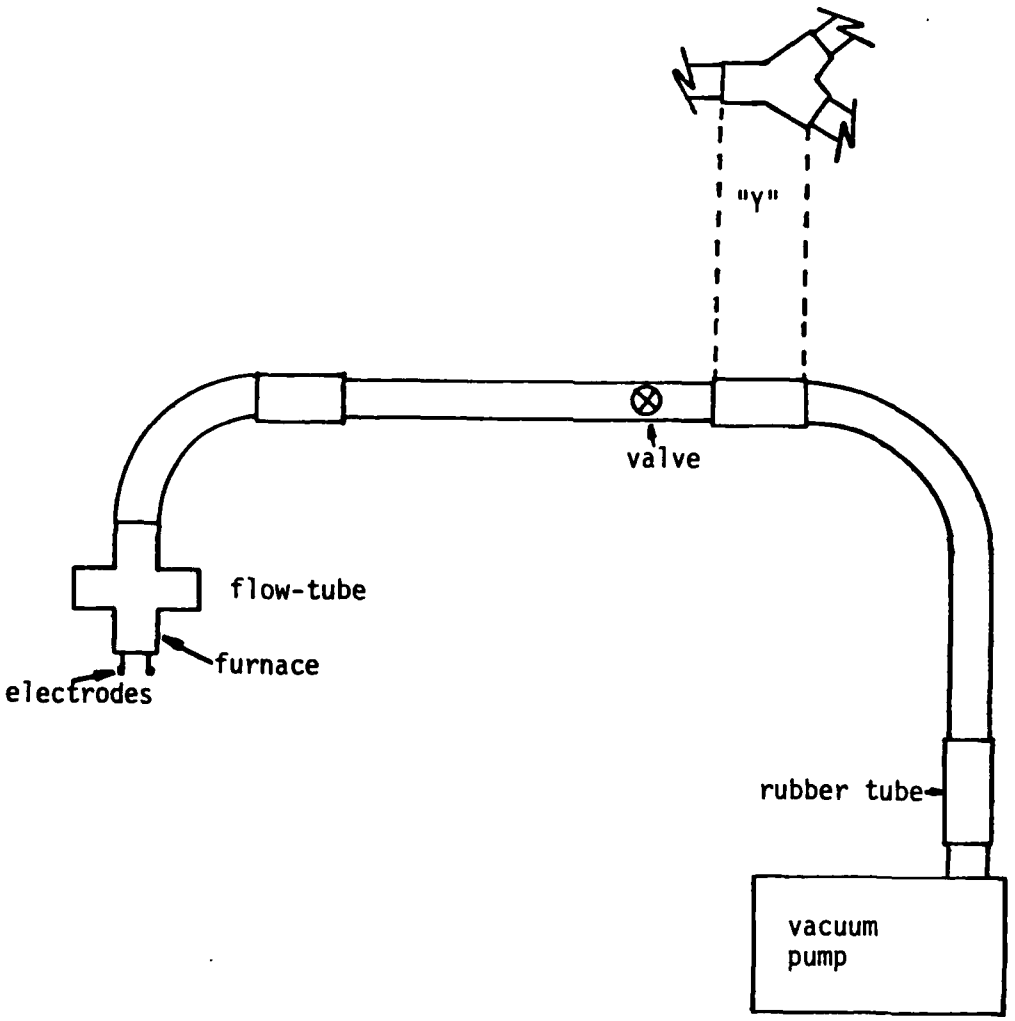

Figure 7. Vacuum System

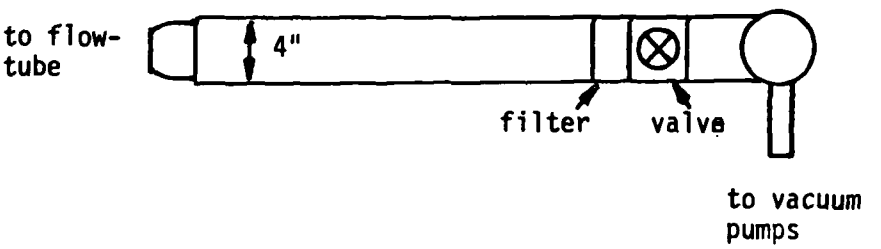

Figure 8. New Vacuum System

2; Flow-Tube System. The flow-tube is constructed of 2 7/8 in. ID stainless steel tube (Alloy Products). The sections are connected together with "C" clamps and rubber O-rings are used between sections to provide a vacuum tight seal. Figure 9 shows the flow-tube system.

The main part of the flow-tube is a 6-way cross. The cross and the back plate are anodized to prevent reflections while taking data. Each arm of the cross extends 3 1/2 in. from the center. A 4 in. extension tube is connected to the port facing the monochromator and is capped with a quartz window. This extension is used to prevent rapid window contamination from the products of the reaction. The other side ports are used to bring in thermocouple wires and the oxygen.

The upper port of the cross is attached to an elbow section. This section is connected to the vacuum system. At the connection point, there is a glass wool particle trap (filter) which prevents the ingestion of the reaction products by the vacuum pumps (21:24).

A water cooled furnace assembly, 4 in. long, is attached to the lower port of the cross. The inside of the furnace is lined with Zirconia cloth to insulate the furnace. The cloth is secured with expandable bands (21:25).

Granular lead is resistively heated in an alumina crucible. The crucible is held by a tungsten coil attached to two brass electrodes. The electrodes are electrically insulated from the furnace by Teflon swage-lock fittings able to hold a vacuum seal. The electrodes are attached to a high current, low voltage power supply (21:25; 11:28).

The lead vapor is transported to the reaction area in the center of the cross with Argon gas. This is done with a 1/2 in. outside diameter (OD) stainless steel chimney and a machined glass ceramic section placed

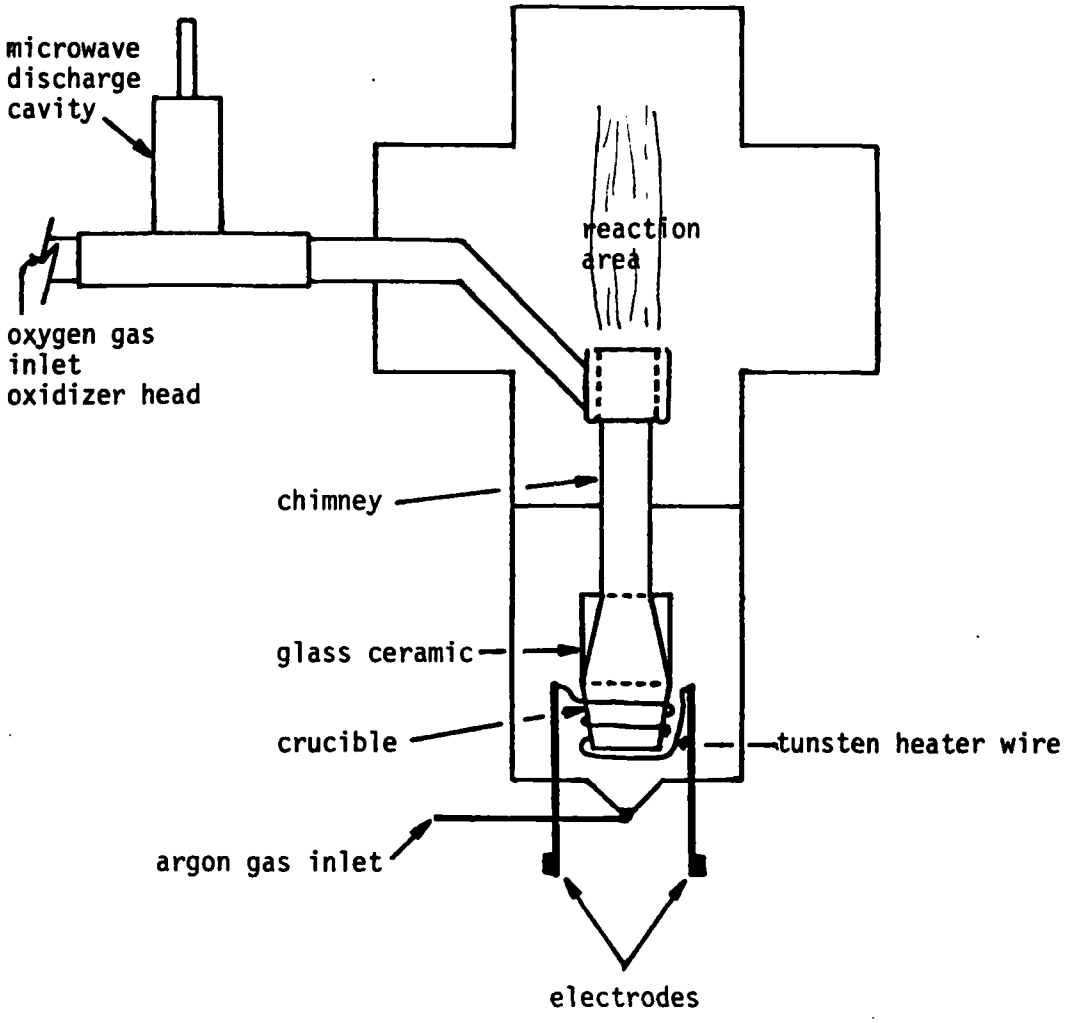

Figure 9. Flow-Tube System

over the crucible. The chimney is held is place by a 1/2 in. Cajon fitting. 4-1/16 in. holes are spaced evenly around the glass ceramic and angled toward the bottom of the crucible. The internal shape of this section is that of a funnel (11:30). The argon gas is brought into the furnace by a tube located between the electrodes.

The mixture of lead vapor and argon gas are brought to the reaction area and combined with the oxygen to produce a flame. The oxygen [$O_2(^1\Delta)$] is led into the reaction area by means of a Pyrex oxidizer head where it mixes with the lead and argon stream. Pyrex is used because of its low quenching coefficient for O_2 ($^1\Delta$). As recommended by Ritchey, a new oxidizer was constructed with holes on the top edge. The oxidizer is a double walled cylinder with the center open. The outer wall is 28 mm and the inner wall is 14 mm. The inner wall has 24- 0.8 mm diameter holes spaced 3 mm apart. 4- 0.8 mm holes are drilled on the top of the oxidizer to form a curtain of gas to prevent flaring of the flame. A curved 13 mm tube is connected to the bottom for an input of the oxygen. The oxidizer is placed over the chimney and forms an extension of it into the flame or reaction regions (21:26,87).

The O_2 ($^1\Delta$) is generated by excitation from a 2450 MHz microwave discharge cavity. O_2 ($^3\Sigma$) is passed through a McCarroll cavity by way of a 13 mm quartz tube (18).

3; Optical Train. The optical train consists of 2 plano-convex lenses of 25 and 50 cm focal length, respectively and a 0.5 m Ebert scanning monochromator (Model 82-020, Jarrel Ash). The light from the flame is focused by the lenses onto the entrance slit of the monochromator. The monochromator is positioned 75 cm from the flame. The two lenses are mounted together in a lens holder with the flat sides touching

and are positioned 25 cm from the flame. The 25 cm lens faces the flame and collects the light. The 50 cm lens focuses the light onto the slit. Three gratings are used having 1180 grooves/mm and blazed at 1900, 3000, and 7500 Å. The entrance and exit slits are linked together and are continuously adjustable from 5 to 400 μm. Eight scaning speeds are available; 2, 5, 10, 20, 50, 125, 200, and 500 Å/min. A high pass optical filter is used with the grating blazed at 7500 Å to block any second order reflections. Appendix B has a transmission curve of this filter.

4; Detection System. The main component of the detection system is the photomultiplier tube (PMT). The PMT, an RCA C31034-02 tube, is mounted on the monochromator with a thermoelectric (Peltier) refrigerated chamber. This chamber is operated at -20°C for these experiments. A water heat exchanger, operated at 15°C, is used to cool the chamber.

The PMT has a spectral response from 2500 to 8500 Å. Appendix C contains the relative spectral response curve and specifications of the PMT. The PMT is powered by an Integrated Detector Assembly (IDA) which is mounted directly on the PMT and the refrigerated chamber. The IDA provides the high voltage and the conditioning electronics in a small package that eliminates noise problems due to cables connecting equipment together. The output is in two forms, analog and digital. The analog output is a voltage proportional to the PMT anode current, 0.1 V/nA. The digital is a photon counting output giving square wave pulses for photons detected using Transistor Transitor Logic (TTL).

5; Recording System. The data is recorded in two ways, either on the strip chart recorder or the Signal Averager (Model 4203 EG&G PAR). The analog data is recorded directly on the strip chart recorder. A low pass

filter is used to eliminate high frequency noise. Appendix D has a diagram of the filter.

The digital or photon counting data is recorded on the Signal Averager (SA) (Model 4203, EG&G PAR). The SA is an all digital multipoint averager having a built-in CRT. The device is used in the multichannel scaling (MCS) mode. The MCS mode is a histogram recorder that collects and stores the number of input pulses for a set dwell time. There are 1024 or 2048 memory locations (channels) used to store information. The SA can be set to collect data at each memory location for a dwell time ranging from 5 μs to 900 ms. The output of the SA can be viewed on the CRT or printed out on a chart recorder. The voltage output of the SA to the chart recorder is reduced by a 1 M ohm voltage divider circuit so a full scale graph can be plotted.

Lead Absorption Spectroscopy

Absorption spectroscopy measurements are done with the same basic set-up as the flow-tube. The additional equipment includes a quartz window, a 10 cm plano-convex lens, and an electrodeless lead lamp. The anodized plate in the area of the cross of the flow-tube is removed and a window installed. The lens is placed next to the window. The lamp is placed at the focal point of the lens so the light entering the flow-tube is collimated. A rectangular (1.2 x 6.0 cm) aperture is placed on the lens to restrict the light to the region were the flame is. The monochromator and the lens assembly (25 and 50 cm focal length), described earlier for the emission studies, are in the same position as for the flow-tube experiment, see figure 10.

The electrodeless lead lamp is operated in a cylinderical microwave (2450 MHz) discharge cavity. The lamp bulb contains lead iodine (yellow in color) and a trace of argon (20). The lamp is heated as recommended by Ball to help stabilize the light output (3:1141). A heater is made with 0.8 mm nichrome wire insulated with 20 guage Teflon tubing. The wire is bent in a U shape and wrapped around a screwdriver shaft to form a loose coil about 7 cm long. The coil is fitted inside a 10 mm ID glass tube. The lamp bulb is placed inside the coil and glass and then inserted into the microwave cavity. A drilled-out rubber stopper is used to hold the lamp in position in the cavity, see figure 11. A low voltage power supply provides the energy to heat the lamp.

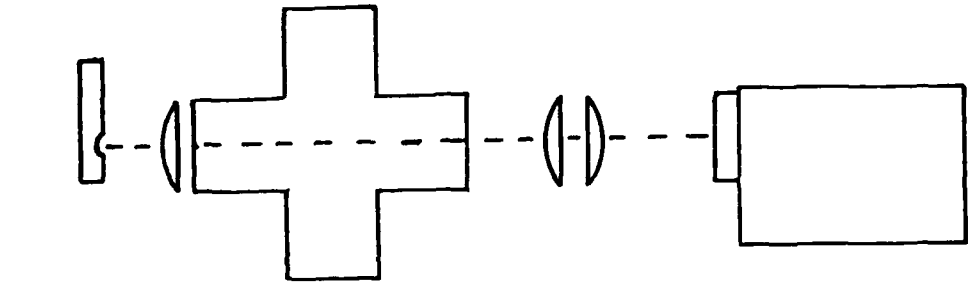

Figure 10. Absorption Spectroscopy Set-Up

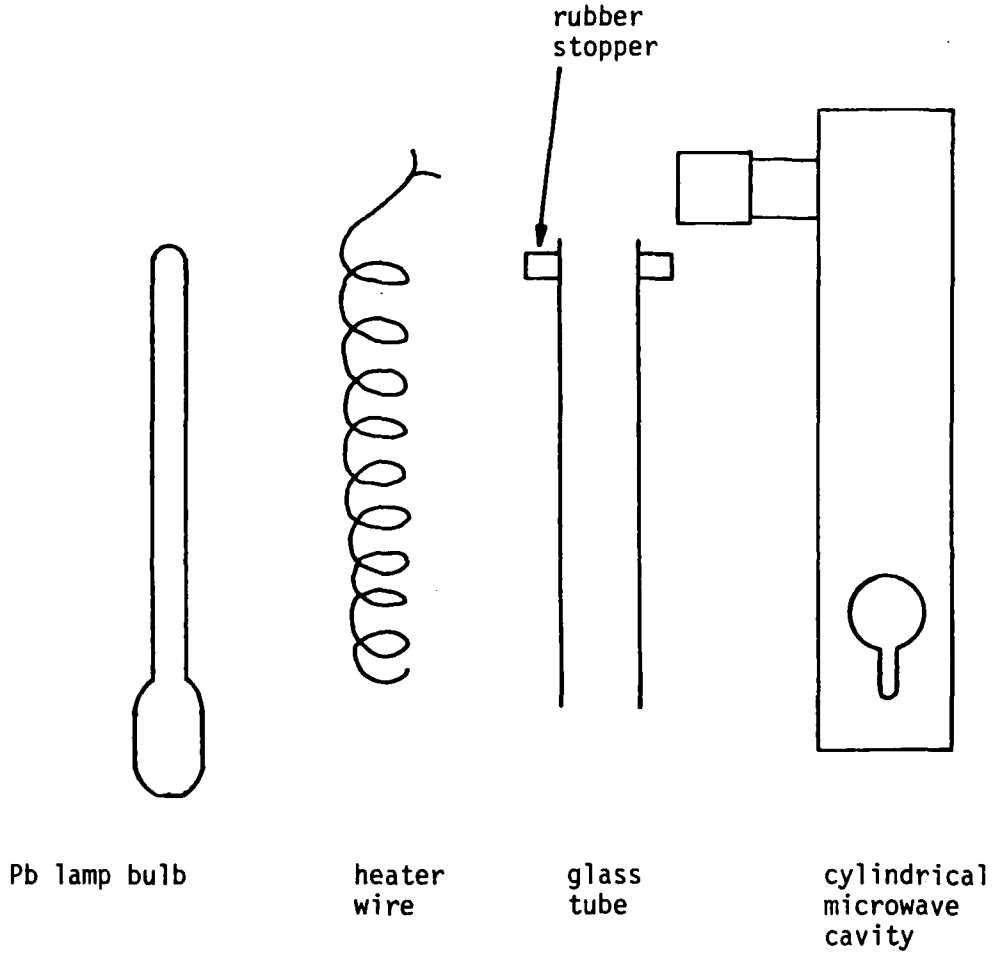

Figure 11. Electrodeless Lamp

IV. Experimental Procedures

Introduction

This section discusses the operation and data collection of the experiments. The start-up and shut-down procedures for the flow-tube system are given in Appendix E. The following topics are discussed: general procedures, alignment, photomutiplier tube optimization, spectral data collection, resolution, and lead absorption.

General Procedures

The entire flow-tube system was cleaned before each data run. The furnace was cleaned of any loose lead particles on the chimney or glass ceramic by scraping with a small metal spatula.

The observation windows were cleaned according to the procedures described. First, the window was cleaned with acetone. Then a thin layer of collodion dissolved in ether was poured on the window and allowed to dry. When dry, the collodion was peeled off the window surface like masking tape. Any deposits remaining on the glass surface adhere to the collodion film and were peeled off with it.

The Pyrex oxidizer was cleaned in a diluted solution of hydrochloric acid and water. After cleaning, the oxidizer was rinsed with water and then with acetone, and finally dried with a slow flow of clean nitrogen gas.

The plasma in the microwave discharge cavity was difficult to maintain. The procedure used to stabilize the cavity was the following. The cavity was cooled by means of a muffin fan which blew on the cavity simultaneously with the passage of compressed air into the cavity through a gas entrance port, see figure 12. The air was obtained from the

building air supply. The flow rate was adjusted so the cavity was just warm to the touch. With this arrangement, the plasma was stable.

Ground state oxygen, still present after going through the microwave discharge cavity, was eliminated by passing the gas over an HgO coating (yellowish brown color) which was on the inside of the quartz tube just past the cavity. The HgO coating was made by flowing oxygen over Hg and passing the gas through the active microwave discharge cavity. This procedure was done once a week for 30 minutes with the power to the cavity at 80 watts and the oxygen pressure set at 1 Torr.

Lead is a toxic element, so caution was used. An exhaust hood was used when working with the lead. The exhaust of the vacuum pumps was routed to the hood.

Alignment

A pen light (Ar or Hg) placed in the center of the oxidizer was used as a light source for the alignment. This arrangement was used to approximate the position of the flame. The lenses and monochromator were then aligned. A sheath with a slit in it was placed on the pen lamp to reduce the intensity of light and a neutral density (ND) filter is placed in front of the monochromator to further decrease the intensity to a level similar to that of the actual flame. The lens holder was modified so the IDA could be used. A 1/2 in. of material was shaved off the side that is next to the IDA. Without this change, the lens holder could not be used since it would touch the IDA and make the alignment impossible.

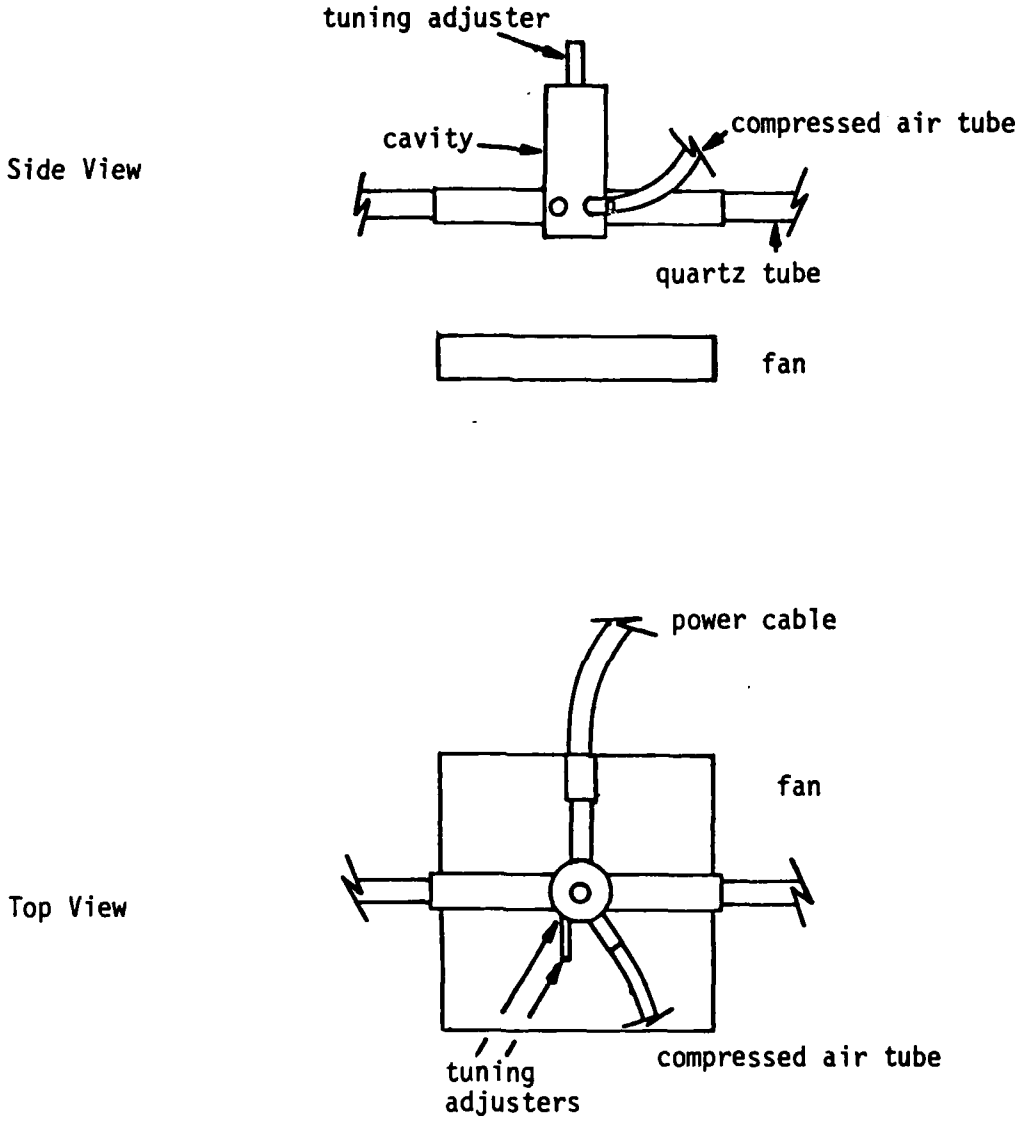

Figure 12. Microwave Discharge Cavity Cooling

Table IV. Gratings and Wavelength Region

Grating Blaze (Å)	Wavelength region (Å)
1900	2000 - 3000
3000	3000 - 4000
7500	7000 - 9000 (use high pass filter)

Four new gratings, blazed at 1900, 3000, 5000, and 7500 Å, were installed in holders. The new gratings were aligned in the monochromator by using the procedures outlined in the manual for the device. Table IV lists the three gratings used for taking the spectral data.

Photomultiplier Tube Optimization

The photomultiplier tube (PMT) used in this experiment had never been used in the photon counting mode. Therefore, the PMT high voltage bias and discriminator threshold were adjusted to give the highest signal-to-noise (S/N) ratio. The discriminator threshold level can be adjusted to set a point, voltage level, where the electronics determine if a photon has hit the cathode. The manufacturer gives a typical dark noise rate of 48 counts per second (cps) at an operating temperature of -20 °C. This was used as a base line to start from in the optimization of the PMT.

The photon count rate was monitored on the signal averager and the photon counter/processor (counter), (Model 1112, EG&G PAR). The dark noise rate was determined with the PMT in total darkness. The count rate is adjusted to an average value of 50 cps by adjusting the discriminator level.

The highest signal-to-noise ratio of the PMT was found by looking at combinations of high voltage and discriminator levels. The voltage was varied from 1.0 to 1.5 KV and the discriminator level was varied from one to the other extremes of the adjustment. A Hg pen lamp was placed in the flame region and was attenuated with a ND filter of 5 to represent the intensity levels of the actual flame. The monochromator was scanned over the 4358 Å line at 125 Å/min with the slit opening set at 15 μm. The data was recorded on the signal averager in the MCS mode with a dwell time set to 500 ms. The S/N ratio is determined by taking the count rate at the 4358 A peak and dividing by the average count rate around the peak, the noise. The highest S/N ratio of 733 is obtained under the following conditions: high voltage, 1200 V; discriminator threshold, aproximately 50 cps - adjustment set to 1/4 turn clock-wise. Figure 13 shows the S/N versus voltage.

Resolution

The resolution of the monochromator is a function of slit width, scan speed, and recording method. The scan speed and the recording are adjusted to give data that can be easily analyzed and can be recorded in a reasonable time period (less than 30 minutes). The slit width is the major factor controlling the resolution, the smaller the better (5 μm minimun slit width).

The dwell time of the signal averager and the scan speed of the monochromator were varied when taking chemiluminescent data. The best combination for taking data in 15 min is a scan speed of 20 Å/min and a dwell time of 900 ms. This combination allowed a wavelength scan of 308 Å to be recorded on the signal averager in 1024 channels; therefore each

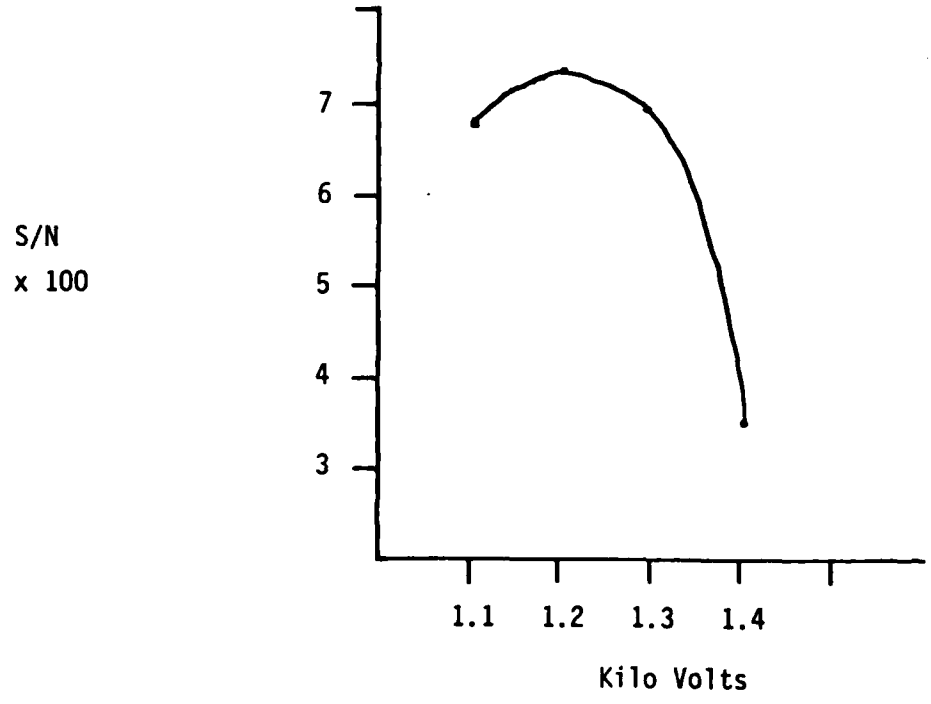

Figure 13. S/N versus PMT High Voltage

TABLE V. Resolution of Detectiom System with 7500 Å Blaze Grating, 1180 grooves/mm

Slit width (μm)	Resolution FWHM (Å)
15	1.8
50	2.1
150	4.2
200	5.1
400	6.9

data point represents a 0.3 Å change. The maximun resolution of the monochromator is 0.2 Å. This "temporal resolution" was considered adequate for the present experiment. The recorded data can be viewed on the CRT or printed out on a chart recorder. The chart recorder was adjusted to print out the data in 45 cm so the linear dispersion is 6.8 Å/cm. The resolution of the total system is determined by scanning over a single spectral line, 7948.2 Å, of a Ar pen lamp. The resolution is given as the full width half maximum (FWHW) of the spectral peak. Table V presents the resolution versus slit width for the grating blazed at 7500 Å.

Spectral Data Collection

Spectral data was taken with the flame at maximum intensity. This operating point was achieved under the following conditions: furnace- 4.5 V, 50 A.; gas pressures- Ar 1.9 Torr, O_2 1.5 Torr. The analog output of the IDA was monitored on the chart recorder when optimizing the optical alignment. The data was recorded in the photon counting mode on the signal averager. Two spectra scans of 308 Å were taken of the same wavelength region, one with and one without calibration lines. The calibra-

tion lines were picked so that at least one line is on each calibration scan. Pen lamps were mounted on an optical rail and moved in the optical path of the monochromator for the calibration scans. The intensities of the lamps were reduced to that of the flame by using opaque sheaths with pin holes. A list of calibration spectral lines and spectral data collection procedures is given in appendix F.

Lead Absorption Spectroscopy

Absorption spectroscopy was preformed to determine the relative concentrations of lead in the vapor stream. The relative intensity of three spectral lines was measured with the lead vapor flowing and with no lead vapor. A Pb electrodeless lamp was used as the light source. It was heated to help stabilize the intensity.

Analog data was taken on the three lines with the the chart recorder. Three data sets were taken in the following sequence: no Pb vapor (furnace off with 2.0 Torr of Ar), Pb vapor (furnace on with 2.0 Torr of Ar), no Pb vapor (furnace off with 2.0 Torr of Ar). Data was taken twice with the furnace off to determine if the lamp remained stable.

Temperature of the lead vapor was measured with an iron-constantan thermocouple. Measurements were taken in two locations, above the heated Pb in the crucible and in the flow-tube just above the Pyrex oxidizer.

V. Results

Introduction

This section contains the observations and analysis of the data collected in performing the experiments. This is divided into four parts. The first part discusses the modifications and general observations of the flow-tube system. Second, the results of the lead absorption spectroscopy are discussed. Third, the spectra and elctronic transition assignments are presented. Finally, the molecular constants obtained from the combination of this data and that of Richey's (9) are presented and compared to that of other researchers.

Flow-Tube Modifications and Observations

Oxidizer Head. The major modification to the flow-tube consists of the substitution of a new oxidizer head as recommended by Ritchey (21:87). The design is presented in the Experimental section. The new head with top holes vertical produced a brighter flame when compared to the old head which had the top holes angled toward the center of the flame region. The flame has a light-blue color of uniform intensity and the shape of a column. Appendix G has pictures of the flame. The old head produced a trianglar shaped flame. Both oxidizers have the problem of the flame spreading when high gas pressures are used. The new oxidizer did produce a flame that did not spread until total pressures (oxygen and argon) of 4 Torr were used. This pressure is the highest that can be used. Higher pressures caused the flame to spread and pulsate.

Table VI. Possible Substances in Flow-Tube System (13,23)

AREA	COLOR OF MATERIAL	SUBSTANCE	TEMPERATURE(°C) (decomposes)
Inside flow-tube walls	brown	PbO_2	290
Oxidizer	brown(cola)	PbO_2	290
	black	PbO_2,Pb_2O	
	yellow	PbO	886
Chimney	red	PbO,Pb_3O_4	500
	yellow	PbO	886
	grey	Pb	328(melts)
	white	Pb	"
Crucible,inside	grey	Pb	328(melts)
	yellow-green	PbO, PbO and WO_2	886
Crucible,outside	blue	WO_2	800(sublimes)

Products of Chemical Reaction. The furnace assembly was always cleaned before an experiment. During this process, many different colored subtances were observed. These colors help identify the type of oxide present. Table VI list the area, color, possible substance, and temperature.

The products or substances found in the flow-tube system all appear to be placed according to the temperature of the particular substance, hot substances in or near the furnace and cool in the flow-tube. Based on the work done in this thesis and that of Glessner (11), temperature ranges have been measured. The results are presented in Table VII.

Table VII. Measured Temperatures in Flow-Tube System

THERMOCOUPLE	LOCATION	TEMPERATURE (°C)
Iron-Constantan	over lead in crucible	600-900
Iron-Constantan Chromel-Alumel	flame region	175-230

The only substance that is not positively identified is the yellow-green material inside the crucible. Initially it was thought that it was due to the combination of yellow lead oxide and a material given off by zirconia cloth. The cloth produced a greenish colored material when heated. The cloth was wrapped around the tungsten heater wire to help insulate it from the furnace walls. The cloth was removed and the yellow-green substance disappeared. The zirconia cloth was left off the wire for the work reported in this thesis. The substance reappeared when a new heater wire was installed. The wire, when heated, produced a dark-blue colored material which is thought to be a tungsten oxide. It is believed that the blue combines with the yellow lead oxide to produce the green. This yellow-green substance did not appear to affect the spectral content of the chemiluminescence.

PMT Dark Noise. The PMT average (mean) dark photon count rate was measured at 43 counts per dwell time of 900 ms on the Signal Averager. The mean deviation was determined to be 7 counts per dwell interval.

Table VIII. Pb(I) Transitions and Appropriate Wavelength

TRANSITION	WAVELENGTH (Å) Calculated (10:66)	Observed
$^3P_2 - {}^3P_o$	9390	9387.1
$^1D_2 - {}^3P_o$	4660	4666.9
$^1S_o - {}^3P_o$	3394	3419.1

Lead Absorption Spectroscopy

Measurements were taken to determine the relative concentrations of excited states of Pb(I). The intensity of three spectral lines were measured with and without the Pb vapor flowing. Table VIII list the transitions and the appropriate wavelengths.

The measurements did indicate a change in intensity of the spectral lines but the light source (Pb electrodeless lamp) did not remain stable throughout the measurements. The data is inconclusive. Therefore another method of taking the measurements is needed.

Spectra

Spectra were obtained and bandhead positions were determined in the regions 2000-4000 Å and 7000-9000 Å. These regions were in the areas where Ritchey (21) had noise problems. The vibrational nature of PbO^* was clearly resolved in the data taken. A picture and a graph of a data run are in Appendices G and H which represent the type of data collected. The data collected and used for analysis was taken with a monochrometer slit width of 150 μm. This slit width provided the best compromise between resolution (small slit width) and intensity (large slit width). Slit widths larger, 200-400 μm, and smaller, 15-50 μm, were used to help determine the location of weak and strong bandheads respectively.

The bandheads were determined at the point where the intensity began to rapidly become stronger than the surrounding data. Bandheads for wavelengths greater than 7000 Å appeared sharp and well defined. For wavelengths less than 4000 Å, the bandheads were not as sharp. The Signal Averager was used to determine the location of most bandheads. Bandheads that were difficult to locate were determined by using the graphs of the data.

The bandhead assignments were made by using the following procedures. A computer program, program SEARCH (11), was used to calculate Deslandres tables for the electronic transitions of PbO. A listing of program SEARCH is in Appendix I. This program used the molecular constants based on Ritchey's data (21; 9). The bandhead positions with their assignments were compared with the experimentally observed bandhead positions. The program printed a list of theoretical bandhead positions and assignments for which occurred within ± 10 Å of the observed bandhead position. These choices were further refined by comparing the relative intensity of the observed bandheads with the previously calculated Franck-Condon factors (19). Final assignments were made by considering the bandhead as a member of a v' or v'' progression.

Where comparison was possible between the bandhead positions observed in this work and that of Ritchey (21) and there was discrepancy, the bandhead position was chosen based on the transition assignment which deviated the least from the calculated assignment from the SEARCH program. Then, this assignment was refined using the procedure described in the previous paragraph.

Finally the bandhead positions were submitted to a least squares analysis using program DUNAM (24). A listing of program DUNAM is in

Appendix I. Molecular constants were calculated and their bandhead positions were also calculated. If an observed bandhead position deviated more than one standard deviation (1σ) from the calculated value, its assignment was re-evaluated. For some cases, weak or ambiguous bands were eliminated but bandhead positions of moderate to strong well defined bands were kept in the list of assignments.

Two assignments were given to a few bandheads. This band overlap was done for the following reasons. The Franck-Condon factors were virtually the same for the two assignments and the difference between the observed and the calculated wave numbers were not greater than 1σ (9.2 cm^{-1}).

Tables IX thru XIII give the data collected which was not observed by Ritchey (21). The listing includes: wavelength, wave number in vacuum, calculated wave number from DUNAM program, differences between the two wave numbers, and transition assignment. The * means there are two transitions assigned to one bandhead. Figures 14, 15 and 16 give the Deslandres table for the transitions between the a - X and A - X states. A few transition assignments made by Ritchey are included. The numbers in parenthesis are the difference between two adjacent wavenumbers.

Molecular Constants. Molecular constants for the X, a, b, A, B, C, C', D, and E states were calculated using a program called DUNAM (24). The data was combined with Richey's data (21) prior to the calculation in order to update the constants. 271 bands were used of which 72 were observed in this work. The bandhead positions with their assigned electronic transitions are entered into the program and a correlated least-squares fit is made to obtain an optimum estimate of the molecular constants. The constants for the a, b, A, B, C, C', and D transitions were calculated without the E state because only seven bandhead positions

were observed for the E state and most of these positions varied more than two from the calculated positions. The molecular constants for the E state were calculated with all the other observed states included. Table XIV lists the molecular constants along with the standard deviations.

Molecular constants previously reported in the literature are given in Table XV. A comparison between the values in the two Tables shows that there is a great deal of variation. Linton and Broida (17), and, Dorko and Ritchey (9; 21) are the only researchers to give a statistical analysis of their data. The data reported in this work and that of Dorko and Ritchey use an un-weighted least-squares analysis. Linton and Broida used a weighted least-squares analysis of their data. The different techniques could explain the variations in the constants.

V' \ V''	2	3	4	5	6	7	8
0		13794 (697) * (476)	13097 (690) * (468)	12407 (674) *	11733 *	*	
1	14963 (693) *	14270 (705) (R)* (466)	13565 * (468)			11532 (473)	*
2	*	14736 (703) *	14033 (683) (481)	13350 (667) (477)	12683 (677) (466)	12006	
3			14514 (687) (R)	13827 (678)	13149		11799 (474)
4							12273
5							
6							13166
7							

All values in cm^{-1}
Numbers in parentheses are differences

* - Franck-Condon factors ≥ 0.1
(R) - Ritchey's data (21)

Figure 14. Deslandres Table for small a to X Transition

V' \ V''	7	8	9	10	11	12	13	14
0	14882 (662)	14220						
		(441)						
1	*	14661 (654) (R)*	14007 (657)	13350				
			(436)	(444)				
2		*	14443 (649) (R)*	13794 (645)	13149			
			(444)	(443)	(438)			
3			14887 (650) (R)	14237 650	13587 (632)	12955 (625)	12330 (622)	11708
					(436)	(439)	(437)	(438)
4					14033 (639)	13394 (627)	12767 (621)	12146
							(435)	(420)
5							13202 (636)	12566

All values in cm^{-1}
Numbers in parentheses are differences

* - Franck-Condon factors ≥ 0.1
(R) - Ritchey's data (21)

Figure 15. Deslandres Table for A to X Transition

V' \ V''	14	15	16	17	18	19
3	11708					
4	(438) 12146					
5	(420) 12566 (597)	11969 (606)	11363			
6		(438) 12407 (608)	(436) 11799 (599)	11200		
7			(434) 12233 (599)	(434) 11634		
8				(430) 12064 (593)	11477	
9				(434) 12498		

All values in cm^{-1}
Numbers in parentheses are differences

Figure 16. Deslandres Table for A to X Transition (continued)

Table IX. Observed PbO Bandheads and Their Assignments

... a - X ...

Observed Wavelength (Å)	Corrected Wave Number (cm^{-1})	Calculated Wave Number (cm^{-1})	Cor-Cal (cm^{-1})	Assignment (v',v'')
7005.9	14269.8	14264.9	-4.9	(1,3)
7124.1	14032.9	14032.9	10.8	(2,4)
7230.5	13826.5	13824.3	-2.2	(3,5)
7247.3 *	13794.4	13786.9	-7.5	(0,3)
7369.9	13565.0	14571.1	6.1	(1,4)
7488.6 *	13349.9	13357.1	7.2	(2,5)
7593.3	13165.9	13176.8	10.9	(6,8)
7602.9 *	13149.2	13144.9	-4.3	(3,6)
7633.4	13096.7	13093.2	-3.5	(0,4)
7882.5	12682.8	12677.8	-5.0	(2,6)
8057.6 *	12407.3	12406.6	-0.7	(0,5)
8146.0	12272.6	12269.7	-2.9	(4,8)
8326.8 *	12006.1	12005.7	-0.4	(2,7)
8380.5	11929.2	11930.7	1.5	(12,14)
8473.2 *	11798.7	11808.0	9.3	(3,8)
8520.4	11733.4	11727.3	-6.1	(0,6)
8669.0	11532.2	11533.1	0.9	(1,7)
8752.2	11422.6	11417.9	-4.7	(5,10)
8837.7 *	11312.1	11316.4	4.3	(12,15)

* means two assignments have been made for one bandhead

Table X. Observed PbO Bandheads and Their Assignments

Observed Wavelength (Å)	Corrected Wave Number (cm^{-1})	Calculated Wave Number (cm^{-1})	Cor-Cal (cm^{-1})	Assignment (v',v'')
		... b - X ...		
7107.2	14066.3	14067.0	0.7	(0,3)
8326.8 *	12006.1	12007.3	1.2	(0,6)
8837.7 *	11312.1	11313.5	1.4	(3,9)
		... A - X ...		
7022.1	14236.9	14234.9	-2.0	(3,10)
7030.2	14220.5	14216.7	-3.8	(0,8)
7137.3	14007.0	14002.7	-4.3	(1,9)
7202.5	13880.2	13884.7	4.5	(8,14)
7247.3 *	13794.4	13794.4	0	(2,10)
7357.9	13587.1	13571.1	6.1	(3,11)
7463.9	13394.1	13394.7	0.6	(4,12)
7488.6 *	13349.9	13352.3	2.4	(1,10)
7536.4	13265.2	13270.4	5.2	(8,15)
7572.5	13202.0	13203.4	1.4	(5,13)
7602.9 *	13149.2	13151.2	2.0	(2,11)
7716.9	12955.0	12955.7	0.7	(3,12)
7830.6	12766.8	12766.0	-0.8	(4,13)
7955.7	12566.1	12581.8	15.7	(5,14)
7999.3	12497.7	12494.7	-3.0	(9,17)

* means two assignments have been made for one bandhead

Table XI. Observed PbO Bandheads and Their Assignments

... A - X ...
(continued)

Observed Wavelength (Å)	Corrected Wave Number (cm^{-1})	Calculated Wave Number (cm^{-1})	Cor-Cal (cm^{-1})	Assignment (v',v'')
8057.6 *	12407.3	12403.4	-3.9	(6,15)
8108.4	12329.5	12327.0	-2.5	(3,13)
8172.5	12232.9	12230.6	-2.3	(7,16)
8231.2	12145.5	12144.4	-1.1	(4,14)
8286.8	12064.0	12063.5	-0.5	(8,17)
8352.9	11968.6	11967.5	-1.1	(5,15)
8473.2 *	11798.7	11796.3	-2.4	(6,16)
8539.0	11707.8	11705.5	-2.3	(3,14)
8593.2	11633.9	11630.8	-3.1	(7,17)
8715.0	11471.3	11470.9	-0.4	(8,18)
8798.6	11362.3	11360.5	-1.8	(5,16)
8926.4	11199.6	11196.5	-3.1	(6,17)
... C' - X ...				
3375.7	29614.7	29595.5	-19.2	(12,1)
3425.9	29180.9	29176.3	-4.0	(11,1)
3769.9	26518.2	26518.0	-0.2	(5,1)
3982.3	25104.2	25097.0	-7.2	(2,1)
4020.8	24863.9	24869.2	5.3	(3,2)

* means two assignments have been made for one bandhead

Table XII. Observed PbO Bandheads and Their Assignments

... D - X ...

Observed Wavelength (Å)	Corrected Wave Number (cm^{-1})	Calculated Wave Number (cm^{-1})	Cor-Cal (cm^{-1})	Assignment (v',v'')
3153.1	31705.8	31743.7	37.9	(3,0)
3202.4	31217.8	31183.3	-34.5	(2,0)
3255.5	30708.8	30682.3	-26.5	(5,3)
3440.3	29058.8	29058.6	-0.2	(2,3)
3590.5	27843.5	27880.6	37.1	(0,3)
3603.6	27742.3	27785.4	43.1	(1,4)
3700.5	27015.3	26998.9	-16.4	(2,6)
3797.9	26322.7	26326.8	4.1	(2,7)
3835.2	26066.8	26105.9	39.1	(4,9)
3905.2	25599.7	25564.6	-35.1	(3,9)
3944.3	25346.0	25334.4	-11.6	(5,11)

Table XIII. Observed PbO Bandheads and Their Assignments

... E - X ...

Observed Wavelength (Å)	Corrected Wave Number (cm^{-1})	Calculated Wave Number (cm^{-1})	Cor-Cal (cm^{-1})	Assignment (v',v'')
3282.3	30458.1	30447.1	-11.0	(4,8)
3302.4	30272.8	30338.6	65.8	(2,7)
3317.1	30137.7	30133.6	-4.1	(0,6)
3392.1	29471.6	29461.6	-10.0	(0,7)
3477.3	28749.7	28796.8	47.1	(0,8)
3569.0	28011.2	27940.4	-70.8	(1,10)
3660.1	27314.2	27297.3	-16.9	(1,11)

Table XIV. Molecular Constants for PbCl

Electronic State	T_e	ωe	$\omega e^X e$
X	0	722.69(0.48)	3.613(0.030)
a	16031.1(4.0)	483.4(1.5)	2.71(0.12)
b	16335.4(6.4)	433.5(5.3)	-0.36(0.90)
A	19876.2(3.3)	445.2(1.5)	0.78(0.15)
B	22303.6(4.0)	491.7(2.0)	0.98(0.21)
C	23794.6(5.6)	550.6(2.3)	5.46(0.19)
C'	24941.9(5.9)	500.1(2.1)	3.40(0.15)
D	30059.3(6.9)	617.7(5.0)	9.56(0.80)
E	34443.0(11.2)	477.4(12.8)	13.0(2.6)

NOTE: Number in parentheses is one standard deviation

All numbers are in cm^{-1}

The constants for the a and A states given by Linton, Dorko, and this work are all within each other's range based on the deviations given. The constants for the other states, calculated in this work, are believed to be the best available. The large number of bands (271) used in the calculations provides a good statistical average of the data. The constants for the D and E states are based on a few bands, 20 and 7, respectively. More data of higher resolution needs to be taken to improve these constants. There are large discrepancies between the observed and the calculated positions and the higher resolution data should clear up these deviations.

Table XV. Previously Reported Molecular Constants for PdO

Electronic State	T_e	ω_e	$\omega_e x_e$	Reference, year
X	—	722.21(0.86)	3.577(0.079)	9, 83
	—	719.3	3.49	11, 82
	—	720.97(0.36) a	3.536(0.025) a	17, 76
	—	721.26	3.53	22, 70
	—	721.6	3.70	4, 61
	—	722.3	3.73	5, 30
a	16031.0(6.4)	482.3(2.7)	2.58(0.25)	9, 83
	16025.9	483.1	2.81	11, 82
	16024.9(1.45)a	481.5(0.7) a	2.45(0.07) a	17, 76
	15912 b	478.4 b	2.5 b	15, 76
b	16339.9(8.8)	428.8(6.7)	-0.69(1.1)	9, 83
	16315 b	441.0 b	—	15, 76
	16379 ± 430	—	—	, 75
A	19874.1(4.3)	445.9(2.0)	0.85(0.21)	9, 83
	19851.4	453.7	2.05	11, 82
	19862.6(1.5) a	444.3(0.8) a	0.54(0.12) a	17, 76
	19721 b	441.9 b	0.20 b	15, 76
	19862.3	444.2	0.46	4, 61
B	22298.5(4.6)	492.7(2.1)	0.98(0.22)	9, 83
	22296.9	495.8	2.22	11, 82
	22166 b	502.0 b	3.8 b	15, 76
	22289.8	496.3	2.33	5, 30
	22289	489	—	4, 61
C	23792.9(5.9)	552.6(2.5)	5.62(0.22)	9, 83
	23820	532	3.9	22, 70
C	24939.2(5.9)	503.4(2.4)	3.62(0.18)	9, 83
	24947	494	3.0	22, 70
D	30083.8(10.1)	589.3(7.9)	5.6(1.4)	9, 83
	30194	530.4	2.9	22, 70
	30197.0	530.6	1.05	4, 30
E	34455	454.1	6.95	22, 70

Note:

- all numbers are in cm^{-1}

- number is parentheses is one standard deviation

a - calculated by a weighted least-squares technique

b - calculated based on ground state constants of (22)

VI. Conclusions and Recommendations

Conclusions.

A flow-tube system has been used to produce a chemiluminescent flame by the reaction of Pb and $O_2(^1\Delta)$. A brighter flame was produced by the use of a new oxider head compared to the old head used previously at AFIT. Also the systems stability was improved by the use of compressed air to cool the microwave cavity used to produce the $O_2(^1\Delta)$.

Seventy-two bandhead and electronic transition assignments were made from the analysis of the spectra observed. This data was combined with Ritchey's data (21) and a set of molecular constants for PbO was calculated. The constants were compared to those of other researchers. The constants calculated for the X, b, B, C, C', D, E electronic states are believed to be the best available. The constants for a and A electronic states are similar to those of Linton and Brodia (17).

Absorption spectroscopy was used to try to determine the relative concentrations of the excited states of Pb in the flow-tube before the reaction with oxygen. The results were inconclusive because of a stability problem with the light source.

Recommendations

Higher Resolution. Higher resolution measurements should be taken of the D and E electronic states so improved molecular constants can be determined. This is possible with the present experimental set-up by using a longer dwell time for the Signal Averager and a slower scan speed for the monochromator. The longer dwell time can be implemented by using an external clock.

Improve the Optical Set-Up. Low light levels make the taking of spectra difficult. Improved spectra could be taken by getting more light into the monochromator. Different lenses and a PMT with a lower wavelength cut-off can help. The response of the PMT begins to roll off at 3000 Å. A cut-off around 2500 Å would improve the response of the system. More light into the monochromator would improve the signal-to-noise of the whole system and a possible way to do this is with cylindrical lenses. Round lenses are presently used and some of the light is lost since the flame is more like a line source instead of a point source.

Improve Vacuum System. An improved vacuum system would help make the flame more stable and allow higher pressures to be used. The present system inhibits the flow by the constriction of the 2 7/8 in. section to 1 1/2 in. A system is being built which will eliminate this problem. The design is in the Experimental Set-Up section. More vacuum pump(s) with a higher capacity will allow higher pressures to be used.

Pb Absorption Spectroscopy. The results of the Pb absorption experiment were inconclusive. They should be done again with an experimental set-up that allows the monitoring of the light source. This will eliminate the need to have a stable light source.

Computer Interface. The Signal Averager (SA) can be connected to a computer. The raw data collected on the SA could be stored and then analyzed on the computer. This would make the job of collecting the data easier and provide a permanent copy of the actual data taken. Presently, the only record of the data taken is the graph and the numbers recorded from the SA.

Bibliography

1. Arnold, S.J. and E.A. Ogryzlo. "Some Reactions Forming $O_2(^1\Delta)$ In The Upper Atmosphere." Canadian Journal of Physics, 45: 2053-2061 (1967).

2. Bachar, J. and S. Rosenwaks. "Reactions of Chemically Produced $O_2(^1\Delta)$ with Pb Atoms." Chemical Physics Letters, 96(5): 526-531 (April 1983).

3. Ball, J. J. "Device for Stabilizing Electrodeless Discharge Lamps." Review of Scientific Instruments, 44(8): 1141 (August 1973).

4. Barrow, R. F. and others. "Rotational Analysis of Absorption Bands of Lead Monoxide." Nature, 191: 374-375 (July 22. 1961).

5. Bloomenthal, S. "Vibrational Quantum Analysis and Isotope Effect for the Lead Oxide Band Spectra." Physical Review, 35: 34-45 (January 1930).

6. Case, C.T. and L.S. Pedrotti. Atomic and Molecular Physics. School of Engineering, Air Force Institute of Technology (AU), Wright-Patterson AFB OH

7. Cole, M. and Ryer, D. "Cooling PM Tubes for Best Spectral Response," Electro-Optical Systems Design: 16-19 (June 1972).

8. Dorko, E.A. and others. "Characterization of the Chemiluminescence Observed During The Reaction Between Lead Vapor and $^3\Sigma O_2$." Chemical Physics Letters, 109(1): 18-23 (August 1984).

9. Dorko, E.A. Personal communications, molecular constants for PbO based on Ritchey's data. September 1984.

10. Garstang, R.H. "Transition Probabilies of Forbidden Lines." Journal of Research of the NBS -A, 68A(1): 61-73 (January-Febuary 1964).

11. Glessner, J. W. Flame Optimization for the Spectroscopic Analysis of the Chemiluminescence from Lead Oxide. MS Thesis. School of Engineering, Air Force Institute of Technology (AU), Wright-Patterson AFB OH, December 1982.

12. Herzberg, G. Spectra of Diatomic Molecules (Second Editon). New York: Van Nostrand Reinhold Company, 1950.

13. Handbook of Chemistry and Physics (64 th Edition). Boca Raton, FL: The Chemical Rubber Co., 1984.

14. Johnson, E.A. Spectroscopy of Selected Diatomic Metal and Metal-Oxide Molecules Using Laser Excited Fluorescence. Phd dissertation. University of California, Santa Barbara, CA, December 1971.

15. Kurylo, M. J., and others. "A Study of the Chemiluminescence of the Pb + O_2 Reactions." Journal of Research of the NBS -A, 80A(2): 167-171 (March-April 1976).

16. Kyom, R.V. A Gas Flow Tube for Spectroscopic Studies. MS Thesis. School of Engineering, Air Force Institute of Technology (AU), Wright-Patterson AFB OH, December 1980.

17. Linton, C. and H.P. Broida. "Chemiluminescence Spectra of PbO Reactions of Pb Atoms." Journal of Molecular Spectroscopy, 62: 396-415 (1976).

18. McCarroll, B. "An Improved Microwave Discharge Cavity for 2450 MHz," Review of Scientific Instruments, 41: 279-280 (1970).

19. Pow, J.J. Development of Computer Routines to Perform a Comprehensive Analysis of Spectroscopic Data from Diatomic Molecules. MS Thesis. School of Engineering, Air Force Institute of Technology (AU), Wright-Patterson AFB OH, December 1983.

20. Reader, J. Personal communication. Opthos Instruments Inc. 20 September 1984.

21. Ritchey, C. M. Spectroscopy and Kinetics of Lead Oxide Chemiluminescence. MS Thesis. School of Engineering, Air Force Institute of Technology (AU), Wright-Patterson AFB OH, December 1983.

22. Rosen, B. Spectroscopic Data Relative to Diatomic Molecules. New York: Pergamon Press, 1970.

23. Samsonov, G. V. The Oxide Handbook. New York: IFI/Plenum, 1973.

24. Skankland, D. G. Program DUNAM. School of Engineering, Air Force Institute of Technology (AU), Wright-Patterson AFB OH, 1983.

25. Suchard, S.N. Spectroscopic Data for Heteronuclear Diatomic Molecules, Vol II. Plenum Publications, 1975.

26. Wasserman, H.H. and R.W. Murray. Singlet Oxygen. New York: Academic Press, 1979.

Appendix A

EQUIPMENT AND MATERIAL LIST

OPTICAL-EQUIPMENT

Quartz windows 3 1/2 in., Supersil
Lenses, U.V. grade fused silica, plano-convex, 3 in. diameter
focal length: 500 mm
250 mm
100 mm
Monochrometer, Model 82-020, Jarrel Ash
Neutral density (N.D.)filters: 0.5
2
3
4
Optical filter, high pass; 500nm cutoff
Spectral calibration pen lamps, Oriel Corp.
Argon
Mercury
Lead (Pb) electrodeless lamp, Opthos Instruments Inc.
Polaroid CR-9 land camera

ELECTRICAL EQUIPMENT

Microwave power supply; Model MPG 4M, Opthos Instruments Inc.
Microwave discharge cavities:
cylinderical, for electrodeless lamp
McCarroll,for production of excited state of oxygen
Tesla coil, Cenco
Reistance wire for heating electrodeless lamp; 2 ohm, 75 cm
Tunsten heater wire
Electrodes, 1/4 in. brass; hold tunsten heater wire
Thermocouple wire, iron-constantan
Muffin fan, 4 1/2 in.
High current power supply; 10 volt, 100 amp.
Power supply; 3 amp., Ultek
Water chiller for PMT cooling housing; part no. 331171, Leybold-
Heraeus vacuum products Inc.

ELECTRONIC EQUIPMENT

Photomultiplier tube (PMT);C3103402, RCA
PMT cooling housing & temperature controler;
model TE104TSRF, Produces for Research, Inc.
Integrated detector assembly; Model 1191, EG&G Princton Applied
Research Corp.
Photon Counter/Processor; Model 1112, EG&G Princton Applied
Research Corp.
Signal averager; Model 4203, EG&G Princeton Applied Research Corp.
Strip chart recorder; Model 0-5137-5M, Omega Engineering Inc.
Volt-ohm meter; Model 18T, Simpson Electric Co.

Ampmeter; Model 633, Weston Electric Instruments Corp.
Trendicator(thermocouple temperature reader); Model 400 B1A-0J-C,
Omega Engineering Co.

VACUUM EQUIPMENT

Vacuum pumps; Model 1397, Welch Scientific Co.
Stainless-steel pipe, 2 3/4 in. ID; Alloy Products
Clamps "C", connect stainless-steel pipe together; Alloy Products
Rubber O-rings, vacuum seal between stainless-steel pipe
steel pipe, 1 1/2 in. ID
Ball valve, 1 1/2 in.; VB-150, Consolidated Vacuum
Rubber tubing, conect steel pipe to pumps
Vacuum guage; Model DV-6M, Teledyne Hastings-Raydist
Vacuum guage; Model 100, MKS Baratron
Cruicible, aluminum oxide; R. D. Mathis Co.
Glass ceramic, MACOR; Corning Glass Works
Cajon fittings 1/2 in.
Swage-lock fittings, Teflon; Nacon Industries

MATERIAL

Lead, granular; atomic weight 207.19 (contains less than 3 ppm of
each: Ag, Cu, Fe, As, Bi, Ni) Fisher Scientific Co.
Argon gas; ultra high purity grade, Matheson Co.
Oxygen gas; ultra high purity grade, Matheson Co.
Mercury
Collodion, for cleaning windows
Acetone
Zirconia cloth

Appendix B

Transmission Curve of High-Pass Optical Filter

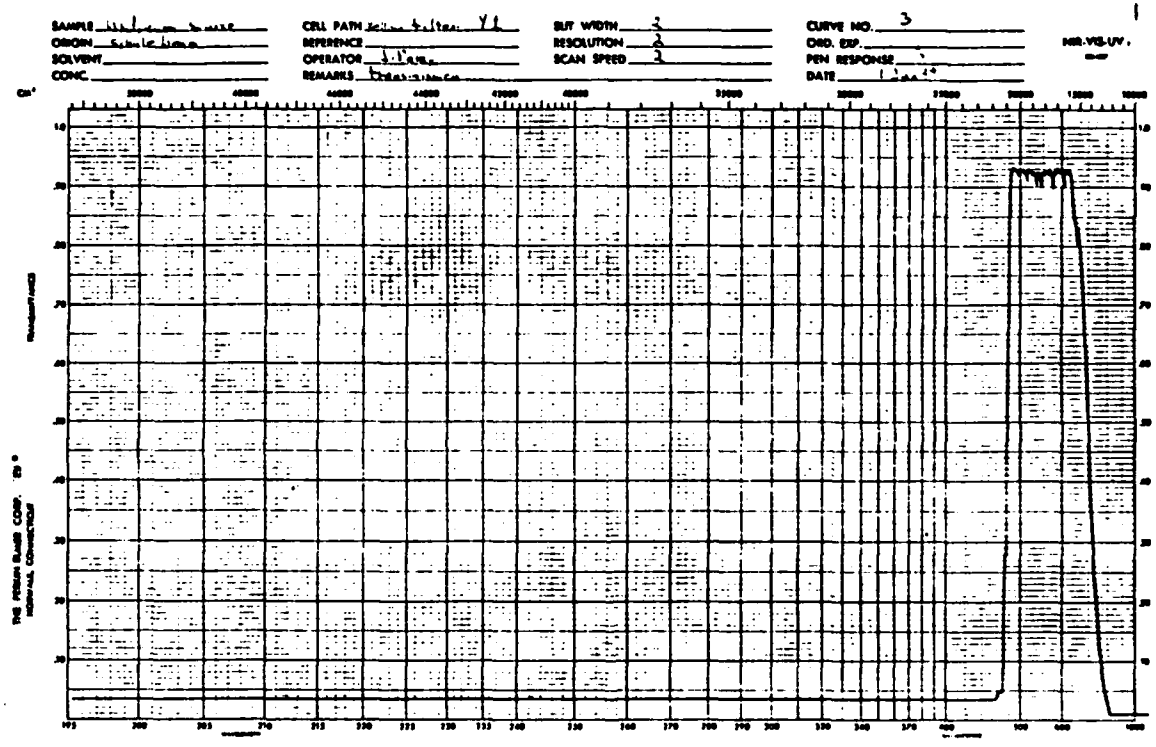

Figure B-1. Transmission Curve of High-Pass Optical Filter - Filter transmits beyond 6000 Å

Appendix C

Photomulpier Tube Information

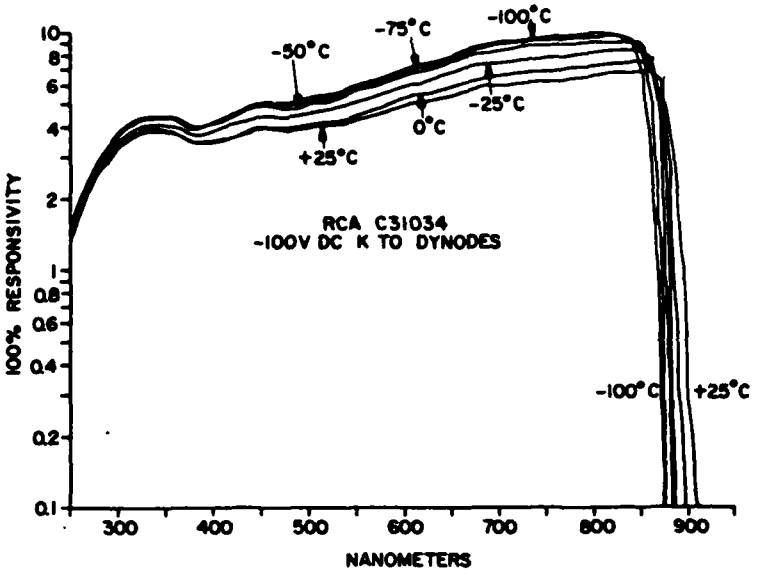

Relative Responsivity vs. Wavelength and Temperature. RCA C31034 Phototube. —100 V dc Cathode to Dynodes.

Figure C-1. PMT Relative Responsivity (7)

Specifications of RCA C31034-02

Cathode Response:

Radiant at 860 nm 26 mA / W

Luminous 360 μA / Ln

Anode Response:

Luminous at 1500 V, 740 A / ln

Photon Counting Mode:

Supply Voltage at 1400 V

22 °C Dark Current 8.2 nA

-30 °C Dark Pulse Summation 10 cps

Appendix D

Low-Pass Filter

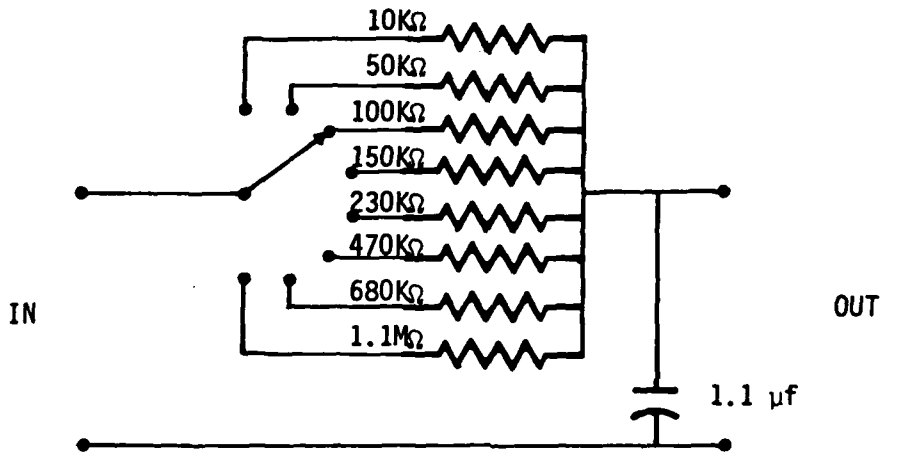

Figure D-1. Low-Pass Filter

Appendix E

Start-up and Shut-down Procedures for Flow-Tube System

Start-up

1. Turn on all electronics at least 30 minutes prior to a run.
2. Fill crucible with lead.
3. Assemble flow-tube system.
4. Close main vacuum valve and vacuum release valve.
5. Start vacuum pumps, one at a time.
6. Open main vacuum valve.
7. Open main valves for gases.
8. Turn on the cooling water to the furnace cooling coils.
9. Turn on the main power switch to the microwave power supply, 3 minute warm-up.
10. When the pressure of the flow-tube system is less than 200 um of Hg, apply power to the furnace heater.
11. Increase voltage to the furnace heater to the desired level, 1 V per 2 minutes (4.5 V).
12. Turn on argon gas, 1 Torr.
13. Turn on oxygen gas, 0.5 Torr.
14. Turn on microwave power switch and increase power to 50 W.
15. Start the plasma in the microwave discharge cavity with the Tesla coil.
16. Adjust the microwave discharge cavity for minumum reflected power (less than 1 W reflected).

    CAUTION: never operate the microwave power supply for more than a few minutes with the SWR greater than 3

$$SWR = \frac{1 + (\text{reflected power} / \text{forward power})^{1/2}}{1 - (\text{reflected power} / \text{forward power})^{1/2}}$$

17. Adjust the microwave power supply for desired power, 80 W.

18. Readjust the microwave discharge cavity for minimum reflected power if neccessary.

19. Turn on muffin fan and compress air for discharge cavity cooling, adjust air pressure so cavity is warm to the touch.

20. Adjust gases for desired flame.

Shut-down

1. Turn off power to furnace heater.

2. Turn microwave power supply to zero output power.

3. Turn off main power to microwave power supply.

4. Turn off oxygen gas.

5. Reduce argon gas to 1 Torr.

6. Allow 15 minutes for the furnace to cool and the reaction produces to be removed from the flow-tube system.

7. Close main vacuum valve.

8. Turn off vacuum pumps.

9. Open vacuum release valve, close when vacuum system is at atmospheric pressure.

10. Turn off cooling water.

11. Turn off argon gas when flow-tube system is at atmospheric pressure.

12. Turn off main valves for gas bottles.

Appendix F

Spectral Data Collection Procedures

1. Set Signal Averager (SA), Model 4203 EG&G PAR, to the MCS mode; adjust dwell time and memory (900 ms; A input, 1024 channels).

2. Determine wavelength region to scan, and spectral calibration lines to be used.

3. Set monochrometer to a wavelength number less than the lower wavelength number of the region of interest.

4. Set monochrometer scan speed (20 Å/minute).

5. Start monochrometer scan.

6. When monochrometer reaches wavelength number of interest, push start button on SA.

7. For calibration run, insert calibration pen lamp in optical path at the appropriate wavelength number.

8. After scan, turn off monochrometer scan switch.

9. Take picture of SA CRT display (F 4, 1/30 sec).

10. Output data to chart recorder.

11. Take data information from SA, counts and position of bandheads.

Spectral Calibration Lines

Wavelength Region(Å)	Source, pen lamp	Spectral Line(Å)
2000-4000	Hg	3125.7
		3341.5
		3650.2
		4046.6
7000-9000	Ar	7067.2
		7272.9
		7384.9
		7503.8
		7635.1
		7723.8
		7948.2
		8115.3
		8264.5
		8408.2

Appendix G

Pictures of Flow-Tube and Spectra

Figure G-1. Flame: Tri-X film; exposure F 4, 8 s

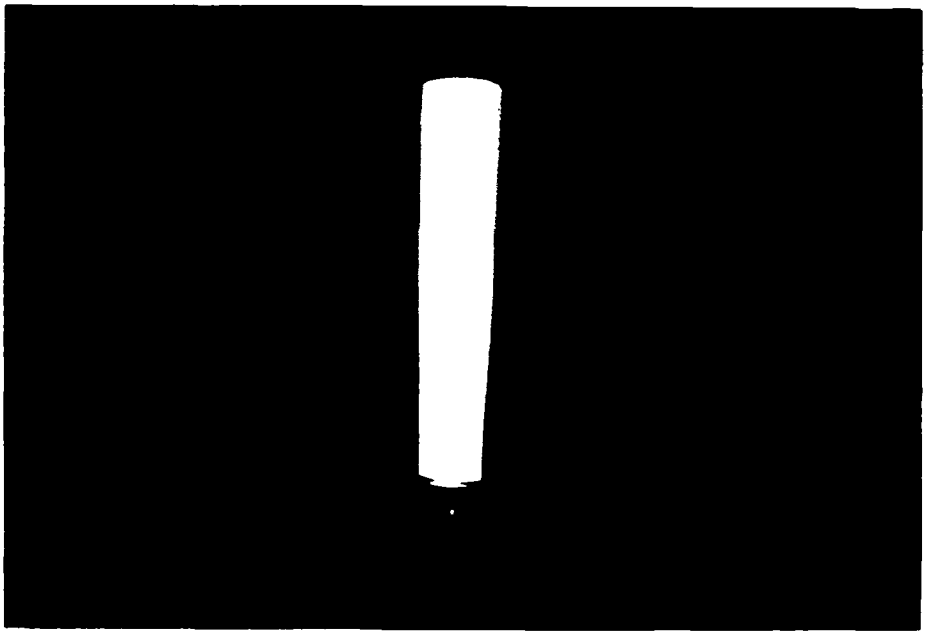

Figure G-2. Flame; Tri-X film; exposure F 4, 1 s

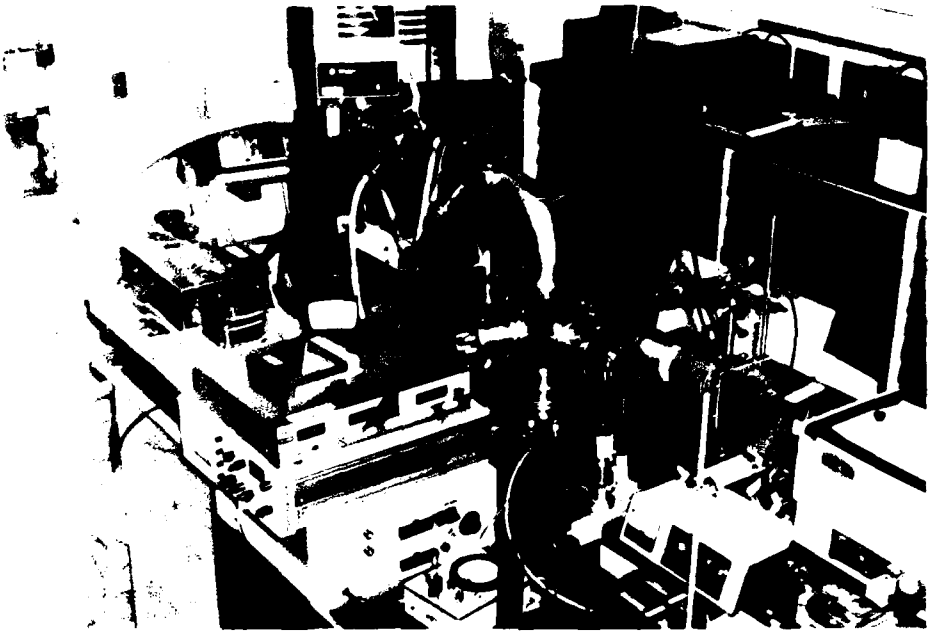

Figure G-3. Flow-Tube System

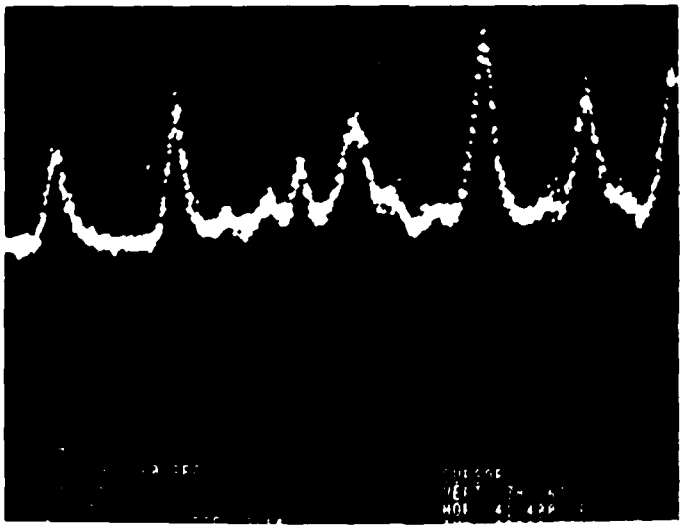

Figure G-4. Spectra 3200 - 3508 Å

Appendix H

Spectral Data 3200 - 3508 Å

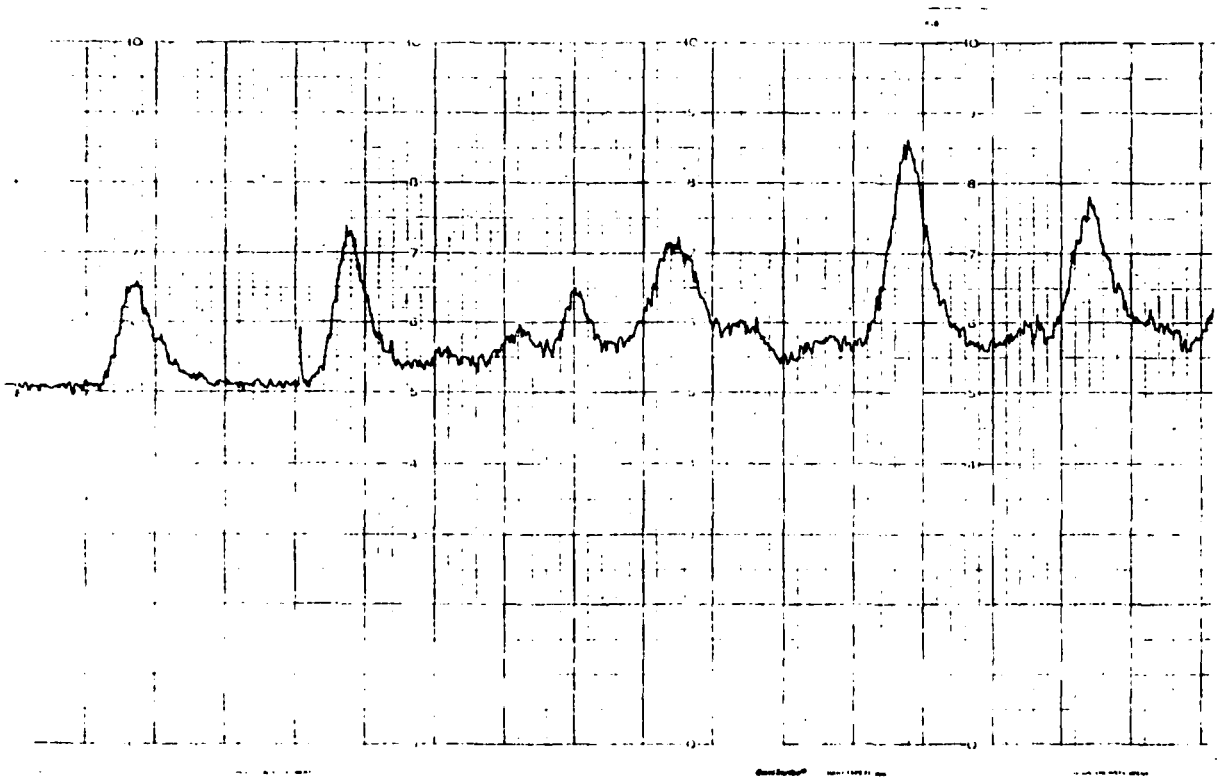

Figure H-1. Spectral Data 3200 - 3508 Å

Appendix I

Computer Programs

```
c          ***     PROGRAM  SEARCH     ***
c
c       This program matches spectra lines to those from a
c       Deslanters Table, and makes corrections to the wavelength
c       numbers for air to vacuum.
c       must update the number of data points (dp) for each run;
c       wl(dp), energy(dp), m=dp
c       The output of this program will be put on file 'searchout'
c         -----
c
      REAL wl(100),wl12(8,21,21),tel(8),wel(8),wexel(8)
      REAL we2(8),wexe2(8),delta,ww,dwl,energy(100)
      CHARACTER tr(8)*2,source*25
      m=100
c
c     ** Initialize
c        delta, is the +- angstom search range
c        Source, is where the data came from
c
      delta=10.
      source='DURAY'
      DATA (tr(i),i=1,8)/'sa','sb',' A',' B',' C','Cp',' D',' E'/
c
c     ** small a-x transition,Ritchey
c
      DATA tel(1),wel(1),wexel(1)/16030.9,482.335,2.573/
      DATA we2(1),wexe2(1)/722.132,3.578/
c
c     ** small b-x transition,Ritchey
c
      DATA tel(2),wel(2),wexel(2)/16340.8,427.928,-0.9482/
      DATA we2(2),wexe2(2)/722.132,3.578/
c
c     ** large A-x transition,Ritchey
c
      DATA tel(3),wel(3),wexel(3)/19873.7,445.815,0.8357/
      DATA we2(3),wexe2(3)/722.132,3.578/
c
c     ** large B-x transition,Ritchey
c
      DATA tel(4),wel(4),wexel(4)/22298.6,492.939,1.0297/
      DATA we2(4),wexe2(4)/722.132,3.578/
c
c     ** large  C-x transition,Ritchey
c
      DATA tel(5),wel(5),wexel(5)/23793.6,552.289,5.6006/
      DATA we2(5),wexe2(5)/722.132,3.578/
c
c     ** large Cp-x transition,Ritchey
c
      DATA tel(6),wel(6),wexel(6)/24938.9,501.601,3.4870/
      DATA we2(6),wexe2(6)/722.132,3.578/
c
c     ** large D-x transition,Ritchey
c
      DATA tel(7),wel(7),wexel(7)/30083.0,594.792,6.5847/
      DATA we2(7),wexe2(7)/722.132,3.578/
c
c     ** large E-x transition,Suchard
c
      DATA tel(8),wel(8),wexel(8)/34455.0,454.1,6.95/
      DATA we2(8),wexe2(8)/722.132,3.578/
```

Program Search
(Continued)

```
c     ** input raw data
c
      OPEN (UNIT=13,FILE='searchfor')
      PRINT*,'INPUT DATA , wavelength in angstroms'
      PRINT 11Ø,m
11Ø   FORMAT(' This program looks for this many data points ',I3)
      PRINT*,'Enter each data point then press <return> ?'
      PRINT 12Ø,m
12Ø   FORMAT(' Enter Ø to stop before ',I3)
      DO 1Ø 1=1,m
       PRINT*,'Enter data point',1,'of',m
       READ(5,*) wl(1)
       IF (wl(1).EQ.Ø) GO TO 13Ø
1Ø     CONTINUE
      GO TO 14Ø
13Ø   m=1-1
c
c     ** calculate Deslanters Table
c
14Ø   DO 2Ø i=1,8
      DO 3Ø j=1,21
      DO 4Ø k=1,21
        ww=te1(i)+we1(i)*(j-.5)-wexe1(i)*(j-.5)**2-we2(i)*(k-.5)+
     c  wexe2(i)*(k-.5)**2
        ww=(1Ø**8)/ww
        w112(i,j,k)=(FLOAT(INT(1Ø.*ww+.5)))/1Ø.
4Ø    CONTINUE
3Ø    CONTINUE
2Ø    CONTINUE
c
c     ** print out heading
c
      WRITE (13,3ØØ)
      WRITE (13,31Ø)
      WRITE (13,32Ø)
      WRITE (13,33Ø) source
      WRITE (13,34Ø)
      WRITE (13,35Ø)
      WRITE (13,36Ø)
3ØØ   FORMAT (' ')
31Ø   FORMAT ('          ---  DESLANTERS TABLE SEARCH  ---')
32Ø   FORMAT (' ')
33Ø   FORMAT ('            Data is from ',A25)
34Ø   FORMAT (' ')
35Ø   FORMAT ('DATA WL TABLE WL    DIFF    TRANS')
36Ø   FORMAT (' ')
c
c     ** search the table for matches
c
      DO 5Ø 1=1,m
       PRINT*,'running',1
        WRITE (13,2ØØ) wl(1)
2ØØ     FORMAT (F6.1)
        wl(1)=wl(1)*1.ØØØ2726+154.5/wl(1)
        wl(1)=(FLOAT(INT(1Ø.*wl(1)+.5)))/1Ø.
        WRITE (13,21Ø) wl(1)
21Ø     FORMAT (F6.1)
        energy(1)=1.Ø/wl(1)*1Ø**8
        energy(1)=(FLOAT(INT(1Ø.*energy(1)+.5)))/1Ø.
        WRITE (13,22Ø) energy(1)
22Ø     FORMAT (F7.1,' cm-1')
        WRITE(13,23Ø)
23Ø     FORMAT (' ')
         DO 6Ø i=1,8
```

Program Search
(Continued)

```
            DO 7Ø j=1,21
             DO 8Ø k=1,21
              1j=j-1
              1k=k-1
              dw1=w1(1)-w112(1,j,k)
              IF(dw1.LT.Ø.Ø) GO TO 1ØØ
              dw1=(FLOAT(INT(1Ø.*dw1+.5)))/1Ø.
              GO TO 9Ø
1ØØ           dw1=(FLOAT(INT(1Ø.*dw1-.5)))/1Ø.
9Ø            IF(ABS(dw1).LE.delta)WRITE (13,24Ø) w112(1,j,k),dw1,tr(1),1j
     +,1k
24Ø           FORMAT('          ',F6.1,'   ',F5.1,'   ',A2,'(',I2,',',I2,
     +')')
8Ø    CONTINUE
7Ø    CONTINUE
6Ø    CONTINUE
5Ø    CONTINUE

      CLOSE (UNIT=13)
      PRINT*,'The end'
      stop
      end
```

Program Dunam

```
10 OCT 84 13:04:46   MMNIS FORTRAN 77 SAU OPTIMIZING COMPILER     01414-00
 MODULE NAME:  MAIN
C      PROGRAM DUNAM
       DIMENSION Z(3,9),A(3,9),B(3,9),VR(400)
       REAL NU
C      DIMENSION Z(#OFTERMS,#OFELECTRONICLEVELS)=Z(MP,LL)
C      DIMENSION ZZ((MP*LL)*(MP*LL+1)/2)
       IN(I,J)=J+I*(I-1)/2
       MP=3
       LL=9
       PRINT100
 100   FORMAT(1H1)
       ML=MP*LL-1
       MZ=ML*(ML+1)/2
       CALL ZERO(B,1,ML)
       CALL ZERO(VR,1,MZ)
       SU=0.
       N=0
C      CALCULATE LINE CONTRIBUTIONS TO MATRICES VR AND A
 11    READ(12,99,END=73)NL,W,NP,VP,ND,VD
       CALL ACC(NL,W,NP,VP,ND,VD,MP,LL,Z,VR,B,SU)
       N=N+1
       GOTO11
C      COMPUTE VR INVERSE FOR VARIANCE COMPUTATION
C      COMPUTE DUNHAM COEFFICIENTS
 73    CALL MOVER(B,1,A(2,1),1,ML)
       A(1,1)=0.
       CALL LINV3F(VR,A(2,1),3,ML,IR)
       PRINT96
       DO4I=1,LL
 4     PRINT98,I,(A(J,I),J=1,MP)
C      COMPUTE G=(N*SIGMA)**2=2*S/N=(SU-B*A)/N
       G=(SU-VPROD(B,1,A(2,1),1,ML,XX))/N
       PRINT98,N,SU,G
C      COMPUTE VARIANCE MATRIX = ZZ**(-1)*G
       CALL VSMULT(VR,1,MZ,G)
C      COMPUTE STANDARD DEVIATIONS AND CORRELATION COEFFICIENTS
       K=0
       DO2I=1,ML
       K=K+I
 2     VR(K)=SQRT(VR(K))
       DO3I=2,ML
       XX=VR(IN(I,I))
       K=I-1
       DO3J=1,K
 3     VR(IN(I,J))=VR(IN(I,J))/(XX*VR(IN(J,J)))
       PRINT95
       CALL PMT(VR,ML)
C      PROGRAM VERIFY
       REWIND12
       S=0.
       SG=SQRT(G)
       DO1I=1,N
       READ(12,99)NU,W,NP,VP,ND,VD
       XP=VP+.5
       XD=VD+.5
       EP=(A(3,NP)*XP+A(2,NP))*XP+A(1,NP)
       ED=(A(3,ND)*XD+A(2,ND))*XD+A(1,ND)
       F=EP-ED
       D=F-NU
       W=SG/ABS(D)
       W=W/(1.+W)
       WRITE(13,99)NU,W,NP,VP,ND,VD
       S=S+W*D*D
 1     PRINT99,NL,W,NP,VP,ND,VD,F,D
       PRINT94,S
       STOP
 99    FORMAT(F10.1,F5.1,I5,F5.0,I5,F5.0,F10.1,F10.3)
 98    FORMAT(I5/(2X,1P10E13.5))
 96    FORMAT(20H1DUNHAM COEFFICIENTS)
 95    FORMAT(32H STD. DEVIATIONS & CORR. COEFF'S)
 94    FORMAT(1P4E13.5)
 93    FORMAT(1P4E13.5)
       END
```

Program Dunam (Continued)

```
      SUBROUTINE AUG(NL,N,NP,MP,MU,MD,MF,LL,Z,ZZ,A,SC)
C     PREPARES THE LEAST SQUARES MATRICES FOR A DUNNAM
C     COEFFICIENT LINE FIT.
      DIMENSION Z(1),A(1),ZZ(1)
      REAL NL
      PL=MP*LL
      MM=PL-1
C     COMPUTING THE AUXILLIARY VECTOR Z
      DO 1 I=1,PL
    1 Z(I)=0.
      NB=(NL-1)*MP
      NA=(NP-1)*MM
      ZB=-Y
      NB=MD+0.5
      ZA=0
      NA=MP+0.5
      DO 2 I=1,MF
      Z(NB+I)=ZB
      Z(NA+1)=ZA
      ZB=ZB+YB
    2 ZA=ZA+XA
C     COMPUTING THE RIGHT-HAND-SIDE CONTRIBUTION
      AA=-NL
      SU=SC+RA*AA
      DO 3 I=2,PL
    3 A(I-1)=A(I-1)+AA*Z(I)
C     COMPUTING THE ZZ-MATRIX CONTRIBUTION
      K=0
      DO 4 I=1,MM
      IF(Z(I+1))5,6,5
    6 K=K+I
      GOTO4
    5 ZI=Z(I+1)
      DO 8 J=1,I
      K=K+1
      IF(Z(J+1))7,8,7
    7 ZZ(K)=ZZ(K)+ZI*Z(J+1)
    8 CONTINUE
    4 CONTINUE
      RETURN
      END
```

```
      SUBROUTINE PRT(VR,PL)
      DIMENSION VR(1)
      JU=0
      DO 5 I=1,PL
      JL=JU+1
      JU=JU+I-1
    5 PRINT 97,(VR(J),J=JL,JU)
      RETURN
   97 FORMAT(2X,1P13E10.2)
      END
```

Vita

Jeffery Paul Duray was born of 30 August 1956 in Revenna, Ohio. He graduated from Elmhurst High School in Fort Wayne, Indiana in 1974 and attended Purdue University from which he received the degree of Bachelor of Science in Physics in May 1978. In April 1979, he graduated and received a commission in the USAF through the Officer Training School, Lackland AFB, Texas. He immediately reported to active duty at the Air Force Wright Aeronuatical Laboratories, Avionics Laboratory, Wright-Patterson AFB, Ohio. While there, he worked on the exploratory development of laser warning systems in the Electronic Warfare Division, Passive Measurements Group. He entered the School of Engineering, Air Force Institute of Technology, in June 1983.

Permanemt Address: 2710 Club Terrace
Fort Wayne, Indiana 46804

Unclassified

SECURITY CLASSIFICATION OF THIS PAGE

REPORT DOCUMENTATION PAGE

1a. REPORT SECURITY CLASSIFICATION: Unclassified	1b. RESTRICTIVE MARKINGS
2a. SECURITY CLASSIFICATION AUTHORITY	3. DISTRIBUTION/AVAILABILITY OF REPORT: Approved for public release; distribution unlimited.
2b. DECLASSIFICATION/DOWNGRADING SCHEDULE	
4. PERFORMING ORGANIZATION REPORT NUMBER(S): AFIT/GEP/PH/84D-2	5. MONITORING ORGANIZATION REPORT NUMBER(S)
6a. NAME OF PERFORMING ORGANIZATION: School of Engineering, Air Force Institute of Tech. / 6b. OFFICE SYMBOL (If applicable): AFIT/EN	7a. NAME OF MONITORING ORGANIZATION
6c. ADDRESS (City, State and ZIP Code): Wright-Patterson AFB, OH 45433	7b. ADDRESS (City, State and ZIP Code)
8a. NAME OF FUNDING/SPONSORING ORGANIZATION / 8b. OFFICE SYMBOL (If applicable)	9. PROCUREMENT INSTRUMENT IDENTIFICATION NUMBER
8c. ADDRESS (City, State and ZIP Code)	10. SOURCE OF FUNDING NOS. — PROGRAM ELEMENT NO. / PROJECT NO. / TASK NO. / WORK UNIT NO.
11. TITLE (Include Security Classification): Spectroscopic Studies of Lead Oxide in a Flow Tube	
12. PERSONAL AUTHOR(S): Jeffery P. Duray, Capt. USAF	
13a. TYPE OF REPORT: MS Thesis / 13b. TIME COVERED: FROM _____ TO _____	14. DATE OF REPORT (Yr., Mo., Day): 84/12/3 / 15. PAGE COUNT: 91
16. SUPPLEMENTARY NOTATION	Approved for public release: IAW AFR 190-17 LYNN E. WOLAVER 2/15/85 Dean for Research and Professional Development Air Force Institute of Technology (ATC) Wright-Patterson AFB OH 45433

17. COSATI CODES		
FIELD	GROUP	SUB. GR.
07	04	
20	06	

18. SUBJECT TERMS (Continue on reverse if necessary and identify by block number): Lead Oxide, Spectroscopy, Molecular Constraints, Chemiluminescence, Flow-Tube Reactor

19. ABSTRACT (Continue on reverse if necessary and identify by block number)

Chemiluminescent flame from lead oxide has been observed in a flow-tube reactor. The chemiluminescence was produced by the reaction of lead vapor with singlet delta oxygen, $O_2(^1\Delta)$, first electronically excited state of oxygen. Spectra was recorded using a monochromator and a photomultiplier tube (PMT). The spectra was recorded from the PMT in the photon counting mode on a Signal Averager (Model 4203 EG&G PAR). The Signal Averager was operated in the multichannel scaling mode which records data in a histogram format.

20. DISTRIBUTION/AVAILABILITY OF ABSTRACT: UNCLASSIFIED/UNLIMITED ☒ SAME AS RPT. ☐ DTIC USERS ☐	21. ABSTRACT SECURITY CLASSIFICATION: Unclassified
22a. NAME OF RESPONSIBLE INDIVIDUAL: Ernest A. Dorko, Professor	22b. TELEPHONE NUMBER (Include Area Code): 513 255-2012 / 22c. OFFICE SYMBOL: AFIT/ENP

DD FORM 1473, 83 APR — EDITION OF 1 JAN 73 IS OBSOLETE.

Unclassified

SECURITY CLASSIFICATION OF THIS PAGE

Analysis of the spectra led to assignments of electronic transitions from a, b, A, C', D, E to the ground state of PbO. Molecular constants were calculated from the combination of this data and previous data taken at the Air Force Institute of Technology. The constants were compared to those of other researchers. ~~The table below lists the~~ molecular constants.

The relative concentrations of excited Pb in the lead vapor were measured by using absorption spectroscopy techniques. The results were inconclusive because of light souce stability problems.

Table of Molecular Constants for PbO

ELECTRONIC STATE	T_e	ω_e	$\omega_e X_e$
X	0	722.69(0.48)	3.613(0.030)
a	16031.1(4.0)	483.4(1.5)	2.71(0.12)
b	16335.4(6.4)	433.5(5.3)	-0.36(0.90)
A	19876.2(3.3)	445.2(1.5)	0.78(0.15)
B	22303.6(4.0)	491.7(2.0)	0.98(0.21)
C	23794.6(5.6)	550.6(2.3)	5.46(0.19)
C'	24941.9(5.9)	500.1(2.1)	3.40(0.15)
D	30059.3(6.9)	617.7(5.0)	9.56(0.80)
E	34443.0(11.2)	477.4(12.8)	13.0(2.6)

All numbers are in cm^{-1}

NOTE: Number in parentheses is one standard deviation

END

FILMED

4-85

DTIC